Calibration & Clinical Measurements in Computed Tomography

-An Evaluation of Different Dosimetric Methods

Eric Grönlund
M.Sc. Thesis, Oslo Spring 2013

Supervisors: Anne Thilander Klang[1]
Hilde Olerud[2,3]
Hans Bjerke[2]

[1]University of Gothenburg, *Department of Radiation Physics*
[2]Norwegian Radiation Protection Authority, *Department of Monitoring and Research*
[3]University of Oslo, *The Institute of Physics*

E-mail: gusgroer@student.gu.se
Phone: 0046-709 837 548 & 0047-983 121 49

The Sahlgrenska Academy

UNIVERSITY OF GOTHENBURG

Abstract

This thesis looked into the established CT dosimetry, highlighting some problems with it. In order to resolve some concerns with it, new dosimetric methods are seemingly beginning to be established. One of these methods based on using point-like detectors instead of the conventionally used pencil ionization chamber.
A calibration procedure for detectors in CT was established. The procedure was more valid for the pencil ionization chamber than for a point-like detector.
This thesis also compared how well a point-like detector could measure the $CTDI_{100}$ compared to the pencil ionization chamber. Measuring in the conventionally used CT phantoms the correspondence was good. But when measuring free in air the correspondence was not completely satisfying.
A dosimetric method to be able to give a size-specific dose estimate based on the $CTDI_{vol}$ was also tested. This method correctly estimated the measured $CTDI_{vol}$ in a small CT phantom. This seems to be a promising method to more correctly know the dose to a patient from a CT scan.

Abbreviations and Terms

CT	Computed Tomography
Axial Scanning	Scanning without table translation during the tube rotation
Helical Scanning	Scanning with table translation during the tube rotation
Pitch (p)	The table translation for one tube rotation during a helical scan divided with the nominal collimation
SFOV	Scan Field of View
CTDI	CT Dose Index
HVL	Half-Value Layer
Homogeneity Coefficient	Ratio of $\frac{\mathrm{HVL}_1}{\mathrm{HVL}_2}$
CTDP	CT Dose Profiler®
CTDI	CT Dose Index
AAPM	American Association of Physicists in Medicine
SSDE	Size-Specific Dose Estimate (According to AAPM 204)
IAEA	International Atomic Energy Agency
IEC	International Electrotechnical Comission
RQR qualities	Radiation qualities in radiation beams emerging from the X-ray source assembly (According to IEC 61267:2005)
RQT qualities	Radiation qualities based on Copper added filter (According to IEC 61267:2005)
CTDI phantoms	Two conventionally used PMMA phantoms with a diameter of 16 cm or 32 cm for measuring the CTDI
QA	Quality Assurance
PSDL	Primary Standards Dosimetry Laboratories
SSDL	Secondary Standards Dosimetry Laboratories
Metrology	The science of Measurement
Aperture	Term synonymously used for a collimator in radiation Metrology
Coverage Factor ('K-factor')	Term used to get an expanded uncertainty within a desired level of confidence
FWHM	Full Width at Half Maxiumum

Contents

1 Introduction **1**
- 1.1 CT Dosimetry . . . 1
- 1.2 Issues about $CTDI_{100}$ . . . 3
  - 1.2.1 Patient size . . . 3
  - 1.2.2 The width of the scanning beam and the phantoms . . . 3
  - 1.2.3 The scanning length . . . 4
- 1.3 New dosimetric techniques for CT . . . 4
- 1.4 Chain of Calibrations . . . 5
- 1.5 Goals for this study . . . 7

2 Materials and Methods **8**
- 2.1 Establishing a calibration procedure for detectors used in CT . . . 8
  - 2.1.1 Acquiring of the Radiation Qualities . . . 8
  - 2.1.2 Calibration of Detectors used in CT . . . 11
  - 2.1.3 Calibration of the detectors . . . 14
  - 2.1.4 Normalization . . . 15
  - 2.1.5 Uncertatinties during calibration . . . 15
- 2.2 Evaluating the Mover system . . . 15
  - 2.2.1 Evaluating the accuracy of measuring the FWHM of beam profiles with the Mover system . . . 15
  - 2.2.2 Evaluate how the plastic tube affects the measured signal with the CTDP 16
- 2.3 Testings of the Detectors on Clinical CT-scanners . . . 17
- 2.4 Evaluate the size dependency of $CTDI_{vol}$ for different phantom sizes . . . 22

3 Results **24**
- 3.1 Calibration of Detectors used in CT . . . 24
- 3.2 Evaluating the Mover system . . . 24
- 3.3 Testings of the Detectors on Clinical CT-scanners . . . 25
- 3.4 Evaluate the size dependency of CTDIvol for different phantom sizes . . . 31

4 Discussion **34**
- 4.1 Calibration of Detectors used in CT . . . 34
  - 4.1.1 Establishing a calibration procedure for detectors used in CT . . . 34
- 4.2 Evaluating the Mover system . . . 35
  - 4.2.1 Evaluate how the plastic tube affects the measured signal with the CTDP 35
  - 4.2.2 Measuring the FWHM . . . 35
- 4.3 Testings of the Detectors on Clinical CT-scanners . . . 36
- 4.4 Evaluate the size dependency of CTDIvol for different phantom sizes . . . 38

5 Conclusion **40**

Acknowledgement **41**

References **42**

Appendix A **i**

1 Introduction

Computed **T**omography (**CT**) is an X-ray imaging technique used for medical diagnostics. A CT scanner utilizes a rotating X-ray source together with detectors on the opposite side of the source. From the collected information images can be reconstructed with computer aided calculations, resulting in tomographic images of the scanned object. CT provides more diagnostic information compared to conventional planar X-ray imaging, since there will not be any overlapping tissue in the images. However CT often gives a significantly higher radiation dose compared with conventional planar X-ray imaging [1]. Also, the frequency of CT examinations is increasing. In 2010 it was stated that the frequency of CT examinations had doubled from 2002 to 2008 and that 80% of the population dose from medical imaging came from CT in the country of Norway [2]. Because CT is an X-ray based imaging technique that increasingly gives a significant contribution to the population dose it is of major importance to have **Q**uality **A**ssurance (QA) procedures with high validity that is up to date with the growing development of new techniques in CT. To be able to make valid measurements for QA procedures the instruments that are used must be calibrated in a standardized and controlled manner. Also of great importance is the validity of the instruments used in the QA procedure. A part of this thesis is to address these issues. This project is about to bring in standardized calibration procedures for detectors that can be used for dosimetric measurements in QA procedures for CT. It is also about to compare and evaluate instruments and methods that can be used in the QA process.

1.1 CT Dosimetry

In CT the most common parameter for estimating the radiation dose is the **CT D**ose **I**ndex (CTDI). CTDI is the integral of air-Kerma along the rotational symmetry axis for the X-ray tube, here denoted z, divided with the number of simultaneously acquired slices, N, of nominal thickness T:

$$\mathrm{CTDI} = \frac{1}{\mathrm{N} \cdot \mathrm{T}} \int_{-L/2}^{+L/2} K(z)\mathrm{d}z \qquad [\mathrm{mGy}] \tag{1}$$

where the L in Eq. 1 defines the length over which the integral is made, ideally the length of integration should be equal or longer than the actual physical air-Kerma profile width. CTDI can be interpreted as the whole air-Kerma profile being deposited in the slice that is defined by the nominal beam collimation.
The following terminology on Dosimetric parameters in CT will be based on the International Standard, IEC 60601-2-44 [3].

CTDI can both be measured free in air and in a CTDI phantom. Regardless of in what one measures it is still air-Kerma that is being measured [4]. The CTDI phantoms most often used so far are cylindrical with a minimum length of 14 cm and made from polymethylmethacrylate (PMMA) with a diameter of 32 cm corresponding for a human body and 16 cm corresponding for a human head [3]. They have a central hole and peripheral holes every 90° 1 cm below the surface, where a detector can be put in the holes to measure the air-Kerma, see Fig. 1.

Most often the detector used is a pencil ionization chamber with an effective measuring length of 100 mm. This means that equation 1 needs to be integrated from $-L/2 = -50$ mm to $+L/2 = +50$ mm and the correct denotation is then CTDI_{100} [3]. The reason for the peripheral holes and the central hole is because then a weighted CTDI_w can be calculated

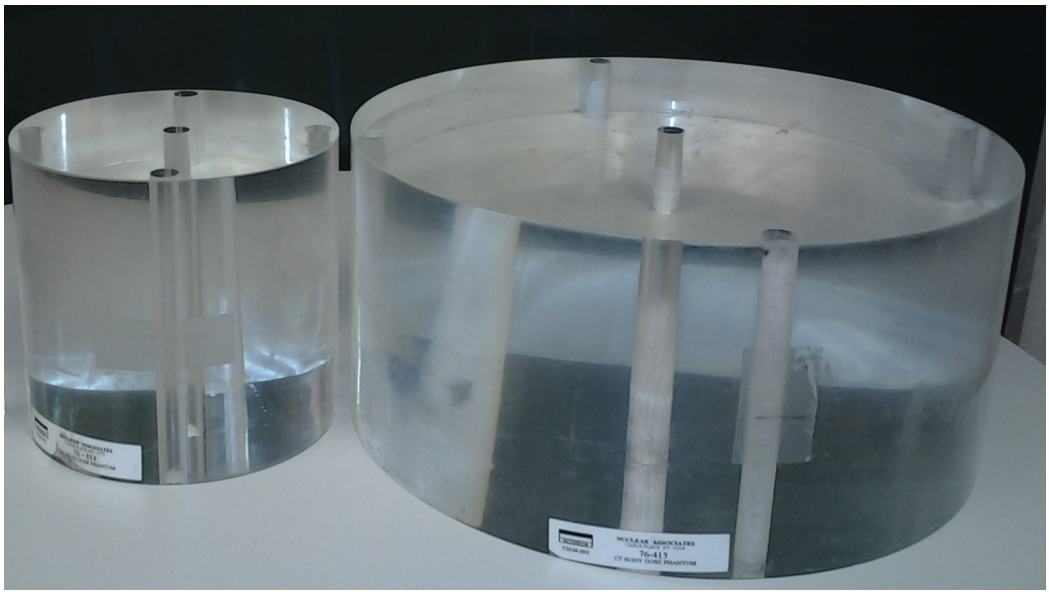

Figure 1: Picture of the two conventionally used CTDI phantoms. The smaller Head phantom with a diameter of 16 cm and the bigger Body phantom with a diameter of 32 cm.

from the measurements [3]:

$$\mathrm{CTDI}_w = \frac{1}{3} \cdot \mathrm{CTDI}_{100,c} + \frac{2}{3} \cdot \mathrm{CTDI}_{100,p} \qquad [\mathrm{mGy}] \tag{2}$$

where $\mathrm{CTDI}_{100,c}$ is the CTDI_{100} from the central hole and $\mathrm{CTDI}_{100,p}$ is the average CTDI_{100} from the peripheral holes. The factors $\frac{2}{3}$ and $\frac{1}{3}$ represents the relative air-Kerma contribution, assuming a linear decrease of the air-Kerma in the CTDI phantoms from the periphery to the centre [5]. CTDI_w can be interpreted as the average air-Kerma in the irradiated cross section.
Further on to take account for any gaps between successive scanning, or take account for successive scanning without table translation, CTDI_{vol} is introduced [3]:

$$\mathrm{CTDI}_{vol} = \begin{cases} \frac{\mathrm{NT}}{\Delta d} \cdot \mathrm{CTDI}_w & \text{axial scanning} \\ \frac{\mathrm{NT}}{\Delta d} \cdot \mathrm{CTDI}_w = \frac{\mathrm{CTDI}_w}{pitch} & \text{helical scanning} \\ n_{tr} \cdot \mathrm{CTDI}_w & \text{without table translation} \end{cases} \qquad [\mathrm{mGy}] \tag{3}$$

where, N, is the number of simultaneously acquired slices of nominal thickness T. For axial sequential scanning Δd is the table translation between the consecutive scans. For helical scanning Δd is the table translation for one tube rotation and the ratio $\frac{\Delta d}{\mathrm{NT}}$ is called the *pitch* [3]. A special case is when there is no table translation, then the CTDI_{vol} is defined as the number of tube rotations, n_{tr}, multiplied with the CTDI_w.
When a patient is scanned in a CT, the scanning goes over the length that will be used for image reconstruction. The scanned length is a bit longer than the reconstructed length. To

get a rendering of the whole radiation exposure across the total scanned length, the term DLP (Dose Length Product) is introduced [3]:

$$\mathrm{DLP} = \begin{cases} \mathrm{CDTI}_{vol} \cdot \Delta d \cdot n_s & \text{axial scanning} \\ \mathrm{CDTI}_{vol} \cdot \mathrm{L} & \text{helical scanning} \\ \mathrm{CTDI}_{vol} \cdot \mathrm{NT} & \text{without table translation} \end{cases} \qquad [\mathrm{mGy} \cdot \mathrm{cm}] \tag{4}$$

where for axial scanning Δd is the table translation between the consecutive scans and n_s is the number of scans in the series. For helical scanning, L, is the total table translation during the series. The special case when no table translation is performed, the length is defined as the number of simultaneously acquired slices, N, of nominal thickness T.

1.2 Issues about CTDI_{100}

1.2.1 Patient size

CTDI_{vol} is defined for the two CTDI phantoms of diameter 16 cm or 32 cm that are at least 14 cm long [3]. Using for example a standard scanning protocol used for scanning chests on adults, the displayed CTDI_{vol} and DLP on the scanner console will be based from the 32 cm Body phantom. This is independently on the actual size of the patient being scanned, since it is only defined for the phantom. However the smaller the patient, keeping the same scanning parameters, the greater the actual radiation exposure of the patient will be. This is something to put extra consideration on, especially when children are being scanned.
To be able to correct the CTDI_{vol} for patients of different sizes the American Association of Physicists in Medicine (AAPM) has published a report to give more correctly **s**ize-**s**pecific **d**ose **e**stimates (SSDE) for different patient sizes based on the CTDI_{vol} [6]. A part of this thesis is to evaluate how accurate these size-specific dose estimates are.

1.2.2 The width of the scanning beam and the phantoms

Today often in the clinic the 100 mm pencil ionization chamber is used for dosimetric measurements of the radiation output from a CT, i.e. measurements of the CTDI_{100}. Measuring over this length is not sufficient to get the total accumulated air-Kerma for in the clinic often used collimations, such as 20-40 mm. Since the air-Kerma profile width due to scattering effects extends beyond 100 mm the measurement will not collect the whole air-Kerma profile. Monte Carlo simulations have shown that CTDI_{100} compared to CTDI_{∞} misses $\sim 60\%$ in Body CTDI phantoms and $\sim 80\%$ in Head CTDI phantoms for 10 mm collimations in the central hole. This percentage or efficiency, was actually approximately the same for 40 mm collimations. For even larger collimations this efficiency was gradually decreasing until it reached 80 mm collimation where it was starting to rapidly decrease even more for larger collimations [7]. Clearly this is an issue that needs to be recognized when optimizing the dosimetry in CT. Especially in that regard that Cone Beam CT scanners, which becomes more common, has beam widths often exceeding these widths, see Fig. 2.
Looking at the CTDI phantoms in this aspect, they are determined to be at least 14 cm long and made from PMMA that has a density of $1.19\,\mathrm{g/cm^3}$. It can be said that 14 cm is not sufficient to simulate how the radiation scattering tails will spread in a real patient, especially as

the material used is not considered to be water equivalent. New ideas says that the phantoms need to be at least 45 cm long [8].

1.2.3 The scanning length

When a patient is being scanned over a certain length, the cumulative dose[1] along this length can be explained as a convolution of the single slice dose profile along the defined length [8, 9]. If the scanning length is at least as long as one single slice physical dose profile an equilibrium value of the accumulated dose value in the centre of the scanning length will be achieved, $D_{eq}(0)$. The actual integrated dose along the scanning length then can be explained as the multiplication of the equilibrium dose with the scanning length L, $D_{eq}(0) \cdot L$. However the problem when measuring with the 100 mm pencil ionization chamber is that one will not measure the whole single slice physical dose profile, which leads to an underestimation of both the equilibrium dose and the integrated dose along the scanning length.

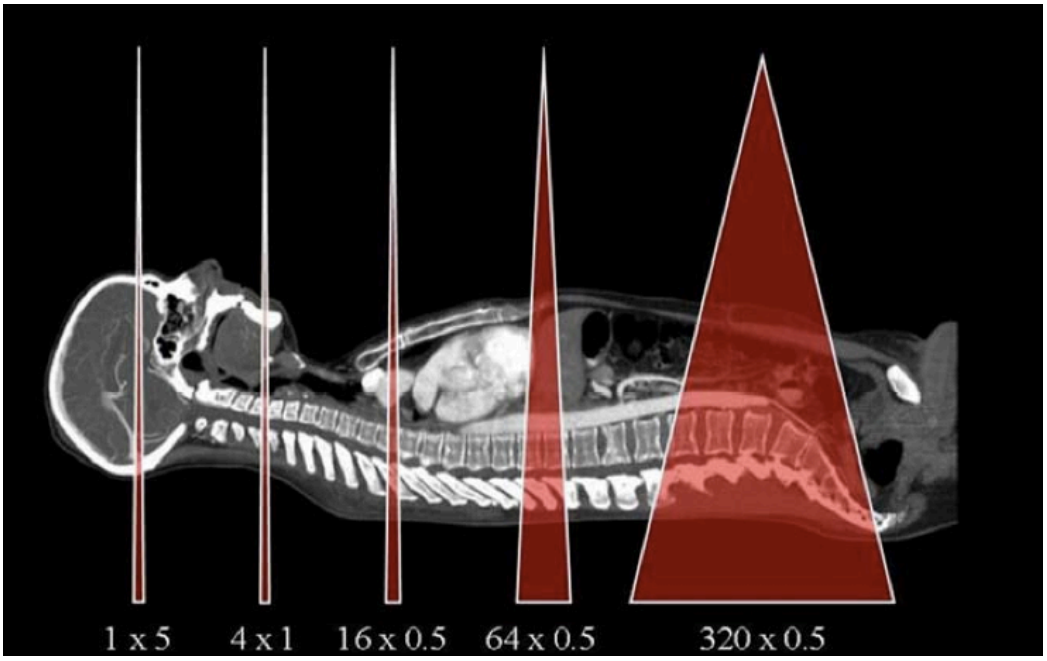

Figure 2: Explanatory picture of the evolution of increasing beam widths in CT. From single slice widths of $4-5$ mm to multi-slice widths of $8-32$ mm and increasing even more to 160 mm widths for Cone Beam CT scanners.
The picture is reproduced with permission by the IAEA:
IAEA publication: International Atomic Energy Agency, Status of Computed Tomography Dosimetry for Wide Cone Beam Scanners, IAEA Human Health Reports 5, IAEA, Vienna (2011), page no. 2.

1.3 New dosimetric techniques for CT

To be able to accommodate the problems with the $CTDI_{100}$, pencil ionization chambers of even longer lengths could be manufactured. However even longer lengths would make them

[1]The article [9] refers to dose, hence the choice of terminology. But the dosimetric unit used in this thesis is air-Kerma if not otherwise stated.

more expensive and more fragile. New ideas of measuring the CTDI in other ways are instead being introduced [8]. These ideas are based on the utilization of a small detector that can be approximated as a point dose detector. To be able to measure the air-Kerma profile during axial scanning the point-like detector can accurately be moved through the beam, free in air or in a phantom, with a mover system. During helical scanning the detector can be placed stationary on the table allowing it to be irradiated, free in air or in a phantom, along a length due to the table movement. A clear advantage of this system is that a picture of the air-Kerma profile can be achieved letting one know how much of the scatter tails is being missed. RTI Electronics AB, have manufactured an angular independent solid state detector, called CT Dose Profiler (CTDP), with a measuring time resolution of 2000 dose values per second and with an effective length of $\sim 250\,\mu$m that can be approximated as a point dose detector. A part of this project is to compare the conventional 100 mm pencil ionization chamber with the CT Dose Profiler. The same company have also manufactured a Mover system that can be used with the CTDP. Also a part of this project is to evaluate the Mover system.

1.4 Chain of Calibrations

Metrology is the science of measurement. The aim in Metrology is to be able to measure physical units as reliable and accurate as possible. An important part in this science is calibrations. A calibration is performed in a way where a measuring instrument is read in conjunction with a known 'normal' or 'reference'. This reference needs to be traceable to another higher level of reference. In figure 3, a very simplified schematic is shown on how the traceability looks for radiation metrology [4]. This schematic is in this project also called, the chain of calibrations. For every step down this hierarchy the uncertainties of measurement grow.

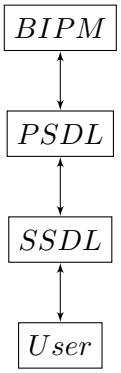

Figure 3: A very simplified schematic of the chain of calibrations for radiation metrology.

Bureau International des Poids et Mesures (BIPM), in Paris has the highest 'authority' in radiation metrology [4]. Primary Standards Dosimetry Laboratories (PSDL) sets the standard to a degree of accuracy as high as possible. The Secondary Standards Dosimetry Laboratories (SSDL) often sets the national standard for physical units when the country not have a PSDL. The SSDL aims to set the standard to a degree of accuracy as high as possible. The SSDL often bridges the gap between the PSDL and the eventual User, for example at the hospital. Within calibration procedures it is important to be able to control all the parameters that will have an influence on the measured signal. Both for the known reference and for the instrument that will be calibrated. Within radiation metrology an important parameter is what radiation

quality one measures in [4]. Therefore radiation qualities for specific applications have been defined. Some specific radiation qualities for applications in CT have been defined by the International Electrotechnical Comission (IEC) [10].
This project was performed in two parts in the chain of calibration, Fig. 3. Namely in the SSDL and in being the User of the instruments. In this project a calibration procedure for detectors used in CT was established. For this procedure some specific radiation qualities needed to be acquired.
The calibration procedure in this study was performed at the Norwegian Radiation Protection Authority (NRPA) in the Secondary Standards Dosimetry Laboratory (SSDL) which is Norway's national reference for the units, Gray (Gy), Becquerel (Bq) and Sievert (Sv).

1.5 Goals for this study

- Establish a standardized calibration procedure for different detectors used in CT
- Evaluate the newly released Mover system
- Compare $CTDI_{100}$ measured clinically with a 100 mm pencil ionization chamber and with the CT Dose Profiler
- Evaluate how accurately $CTDI_{vol}$ can be size corrected

2 Materials and Methods

2.1 Establishing a calibration procedure for detectors used in CT

2.1.1 Acquiring of the Radiation Qualities

In order to establish a standardized calibration procedure for detectors used in CT, some radiation qualities specific for CT called RQT qualities, needed to be acquired. The RQT qualities are based on RQR qualities, which application is in general radiography, but with added copper filtration [4, 10]. RQR qualities only have aluminium filtration.
The radiation qualities that needed to be acquired for this study are defined by the International Electrotechnical Commission (IEC) and the terms, definitions and method for acquiring these radiation qualities are described in the same report [10]. The radiation qualities to be acquired are referred to as RQT 8 IEC 61267:2005, RQT 9 IEC 61267:2005 and RQT 10 IEC 61267:2005, but will be called RQT X further on in this report where X represents 8, 9 or 10, see Tab. 1. It should be noted that the RQT qualities are not defined with a nominal homogeneity coefficient, hence no measurements of that parameter was made.

Table 1: The RQT qualities, with the X-ray tube voltage, nominal added copper filtration in mm Cu, the nominal first **h**alf-**v**alue **l**ayer (HVL) in mm Al and the two different thicknesses of aluminium used when measuring the HVL.

Radiation Quality	X-ray tube voltage [kV]	Nominal added filter [mm Cu]	Nominal first half-value layer [mm Al]	T_1 [mm Al]	T_2 [mm Al]
RQT 8	100	0.20	6.90	6.57	7.10
RQT 9	120	0.25	8.40	8.13	8.64
RQT 10	150	0.30	10.10	9.64	10.64

The measurement arrangement was set up with a Capintec 30cc PM30 Ionization Chamber (serial no. 1232). With help from lasers the center of the Capintec chamber could be placed 100 cm from the focal spot in the X-ray tube (Comet MXR-160/0.4-3.0). The X-ray tube provides a continuos output of the radiation, has a target angle of 20° and an inherent filtration of 0.8 mm Be. A plastic wheel with holes of 5 cm in diameter around the wheel was used to put the filtration material for the radiation quality (Goodfellow, Cambridge Ltd.). The copper and aluminium filtration material was given to have an elemental purity of at least 99.9%. The plastic wheel with its filtration holes was placed 18 cm from the tube focus. Five cm from the filtration hole an in-house constructed mover was placed together with the half-value layer test device. The half-value layer test device consisted of two different aluminium filtration packages, one package with thickness T_1 just below the nominal HVL and one package with thickness T_2 just above the nominal HVL for the quality in mind, see Tab. 1 for the values of T_1 and T_2 for the different radiation qualities and Fig. 4 for the measurement arrangement.

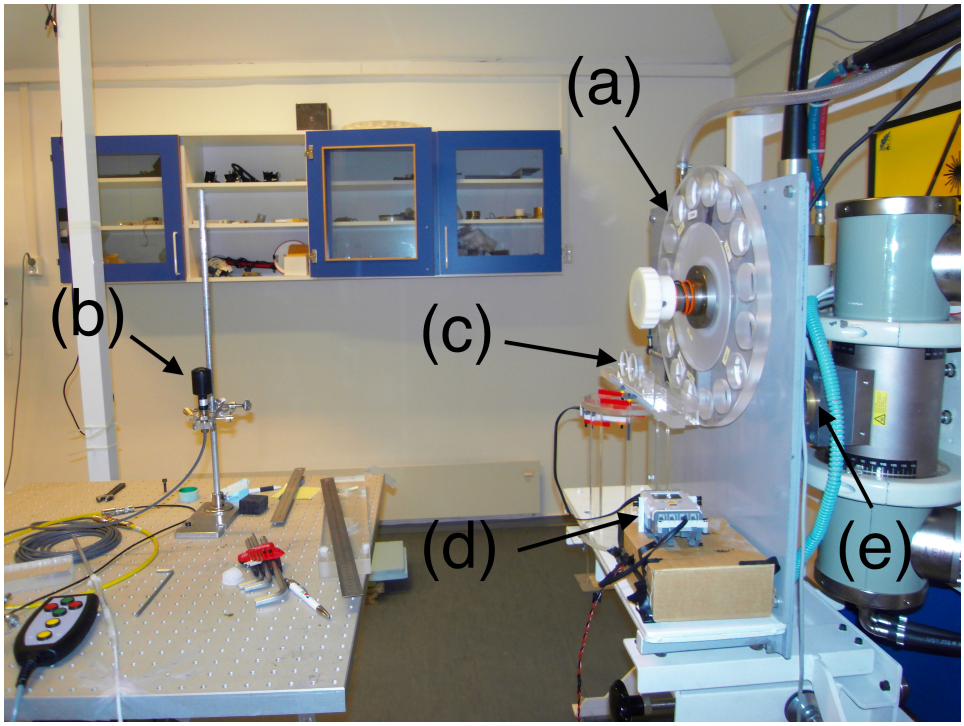

Figure 4: An explanatory picture of the arrangement for acquiring and measuring the HVL for the RQT qualities.
(a) Rotational plastic wheel with holes for the filtration material needed for different radiation qualities.
(b) Capintec 30cc ionization chamber located 100 cm from the tube focus.
(c) The half-value layer test device with the two aluminium packages, one with thickness just below and one with thickness just above the nominal HVL.
(d) In-house constructed mover system for the half-value layer test device.
(e) The X-ray tube.

The X-ray voltage generator (Pantax, HF 320/160) was set to 100 kV and the tube current to 29 mA to acquire the first radiation quality, RQT 8. For RQT 9 the X-ray voltage generator was set to 120 kV and the tube current to 25 mA. For RQT 10 the X-ray voltage generator was set to 150 kV and the tube current to 20 mA. The three qualities were established in the same following way.
The leakage current was measured before any radiation was turned on. The sampling of current from the electrometer was automatically made in a computer program. The sampling was made with 1 second intervals getting the instantaneous current in Ampere 50 times. The average current of the 50 samplings was then calculated, giving the measured current. The estimated standard deviation was also calculated for the 50 samplings. The radiation beam was turned on and a first measurement of the current without any attenuating aluminum was made, giving the measured value $I_{0,1}$. With the radiation beam still on, the in-house constructed mover moved attenuating aluminium with a thickness, T_1 mm, just below the specified nominal HVL into the beam. The current was then measured giving a measured value I_{HVL,T_1}. The mover moved attenuating aluminium with a thickness, T_2 mm, just above

the specified nominal HVL and the current was measured in the same way giving the measured value I_{HVL,T_2}. Lastly the mover moved away the attenuating aluminium out of the beam and the current was measured in the same way as without any attenuating material to see if the X-ray system had drifted in any way, giving the measured value $I_{0,2}$. The average value of the two measured values $I_{0,1}$ and $I_{0,2}$ was calculated giving I_0. Every measured value was temperature and pressure corrected and corrected for the leakage current. The ratio of $I_{HVL,T_1}/\ I_0$ and $I_{HVL,T_2}\ /I_0$ was calculated and these values were plotted on the Y-axis with the corresponding thicknesses of the attenuating aluminum, T_1 and T_2 on the X-axis. The nominal HVL was linearly interpolated in the plot between the values T_1 and T_2 to see what the ratio would be with the nominal HVL, see Fig. 5. If the ratio of the interpolated value for the nominal HVL was between 0.485 – 0.515 the Radiation Quality was considered to be obtained [10]. If the ratio was not between these values the filtration on the plastic wheel was adjusted. If the ratio was too high, added filtration was needed and if the ratio was too low, filtration needed to be removed.

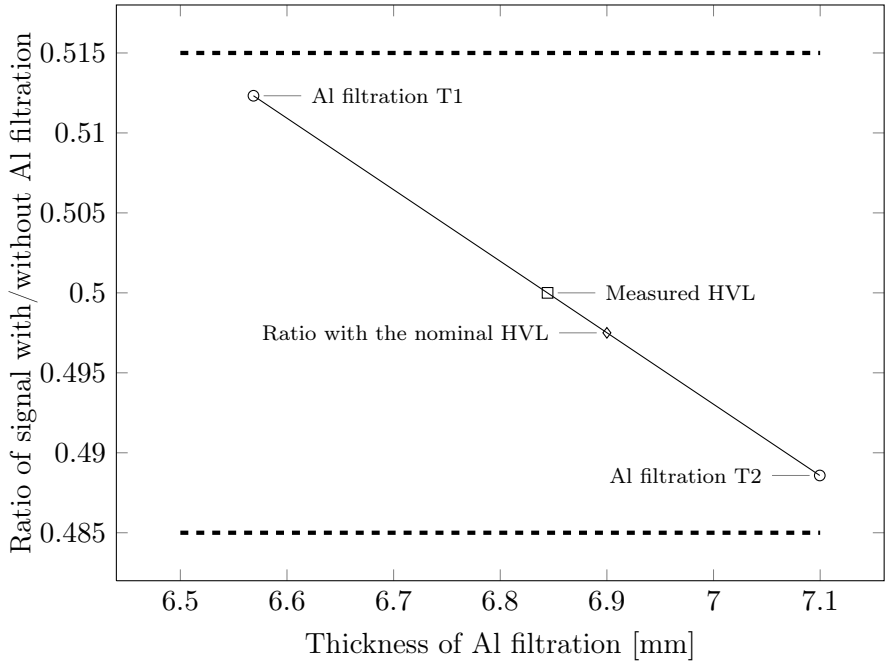

Figure 5: The ratio of the signals $I_{HVL,T_1}/\ I_0$ and $I_{HVL,T_2}/\ I_0$ with the correspondent thicknesses T_1 and T_2 of aluminium filtration (∘). The interpolated value of what the ratio would be with the nominal HVL (◊), the measured HVL where the ratio is 0.5 (□) and the upper and lower limits for what is considered to be acceptable in dotted lines. These are the values when RQT8 was acquired.

2.1.2 Calibration of Detectors used in CT

Two detectors were calibrated, one 100 mm pencil ionization chamber (Radcal®, Model no.10x5-3CT, serial no. 8319) and one semiconductor CT Dose Profiler (CTDP), from RTI Electronics (serial no. DP2-12120084). Calibrations were made in the newly acquired RQT qualities and in RQR qualities already established on the SSDL, see Tab. 2. All radiation qualities were based on IEC 61267:2005 [10].
To be able to calibrate the detectors one must accurately know what the air-Kerma rate for reference is in the correct radiation qualities. The reference air-Kerma rate was determined with help from a reference pencil ionization chamber (DCT 10, IBA Dosimetry, GmbH, serial no. 253). The reference pencil ionization chamber was during this project calibrated at the national metrology institute of The Netherlands, VSL. The calibration procedure was performed by first measuring with the reference pencil chamber[2] in all radiation qualities, Tab. 2. Then turning off the radiation and switch to one of the detectors that would be calibrated. Which was repeated again for the remaining detector. The calibration procedure was performed on two different days to see the stability of the detectors.

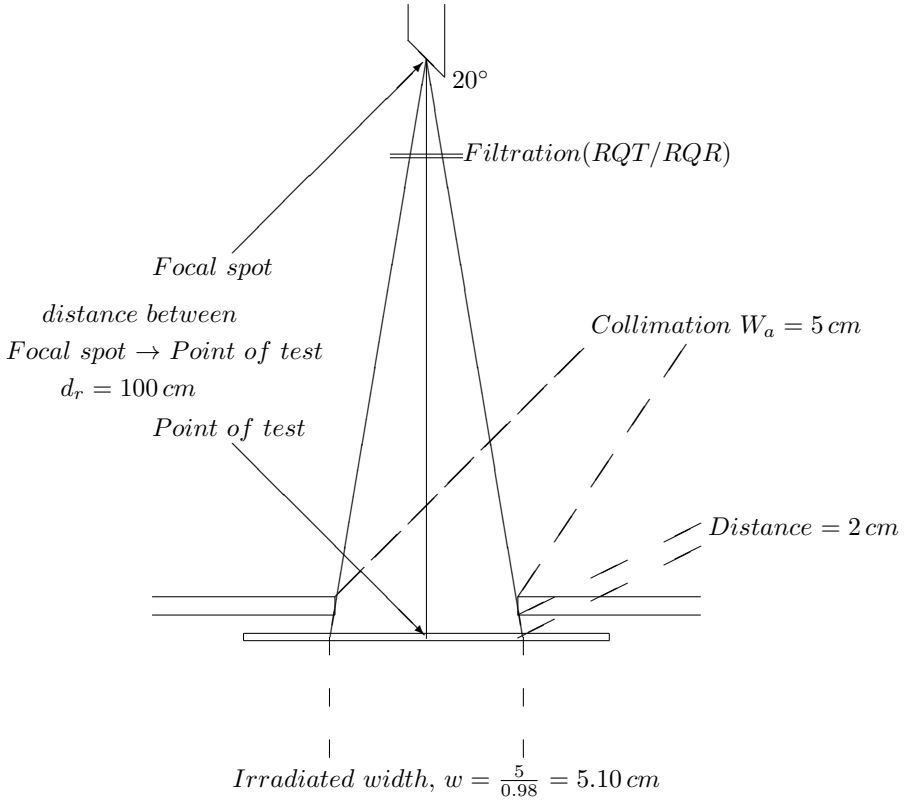

Figure 6: Explanatory drawing of the arrangement for calibration. The anode angle of the X-ray tube was 20°. The exit of the collimation was 98 cm from the focal spot and the point of test was 100 cm from the focal spot. This gave an irradiation width of 5.10 cm. This was the arrangement for all detectors, the reference pencil chamber (DCT 10), the Radcal pencil chamber and the CTDP.

[2]To reduce the length of the terms for the reference pencil ionization chamber and for the Radcal pencil ionization chamber. They will now be called reference pencil chamber and Radcal pencil chamber.

Figure 6 and 7 describes how the calibration measurements for all detectors were made. The measurements for calibration were made with a square aperture, $5 \times 5\,\mathrm{cm}^2$, which was placed so its ending seen from the beams eye view was 98 cm from the tube focus, see Fig. 6. The aperture was first centralized, but then raised 1 cm towards the cathode direction resulting in the field coming out from the aperture more homogeneous. The central point of the chamber was then placed so it was in the center of the aperture and 100 cm from the tube focus i.e. 2 cm from the apertures ending.

Firstly the reference pencil chamber (DCT 10) was irradiated using the different radiation qualities, see Tab. 2, and the current was measured in the same way as with the HVL measurements. Measurements with the reference pencil chamber was repeated two times giving a total irradiation time of 100 seconds. All calibration measurements for all detectors were made with a tube current of 5 mA.

Table 2: The radiation qualities, based on IEC 61267:2005, used for calibration with their respective X-ray tube voltages and their at SSDL measured half-value layer in mm Al. Also noted is the total filtration for each radiation quality. Note that RQR qualities do not have any copper filtration.

Radiation Quality	X-ray tube voltage [kV]	X-ray tube current [mA]	HVL [mm Al]	Total filtration [mm Al] + [mm Cu]
RQT 8	100	5	6.84	3.46 + 0.16
RQT 9	120	5	8.48	3.49 + 0.22
RQT 10	150	5	10.36	3.37 + 0.30
RQR 9	120	5	4.98	4.04 + 0

The measured signal, M_{Ref}, from the reference pencil chamber (DCT 10) was a current with an order of magnitude around 10^{-11} A. To convert the measured current to a reference air-Kerma rate in the specific beam qualities Q, the following relationship was used:

$$\dot{\mathrm{K}}_{Ref,Q} = \frac{M_{Ref} \cdot \mathrm{N}_{KL} \cdot k_p \cdot \mathrm{k}_Q}{w} \qquad [\mathrm{mGy/s}] \tag{5}$$

where $\mathrm{N}_{KL} = 26.13\,\mathrm{mGy} \cdot \mathrm{cm/nC}$ was the calibration coefficient and k_Q corrected for the radiation quality. N_{KL} and k_Q was supplied from the calibration certificate from VSL. k_p was the correction for temperature and pressure. w was the irradiated length of the chamber and was calculated from the following relationship:

$$w = \frac{W_a \cdot d_r}{d_a} \qquad [\mathrm{cm}] \tag{6}$$

where $W_a = 5\,\mathrm{cm}$ was the width of the square aperture, $d_r = 100\,\mathrm{cm}$ was the distance between the focal spot and the point of test and $d_a = 98\,\mathrm{cm}$ was the distance between the focal spot and the exit of the square aperture, see Fig. 6. The irradiated length, w in cm, of the pencil chamber was calculated according to the geometrical relationship of similarity and also as described by IAEA 457 on how pencil ionization chambers should be calibrated [4].

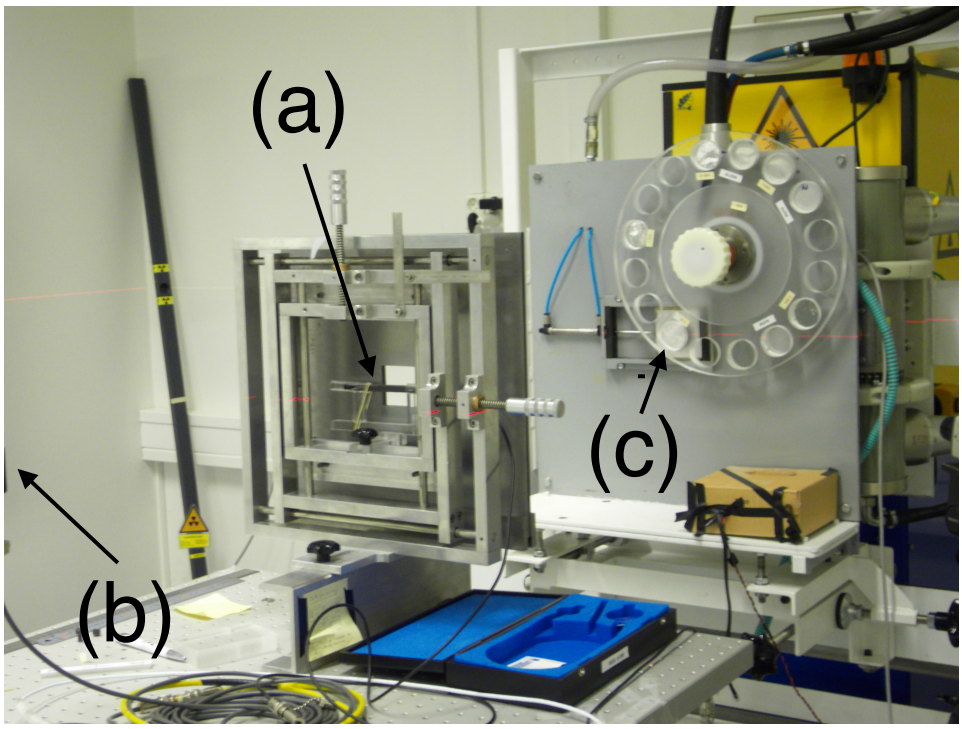

Figure 7: An explanatory picture of the arrangement for how calibrations of the detectors were performed.
(a) The reference pencil chamber, IBA DCT 10, 100 cm from the tube focus put on a plastic holder that is fastened on a stand used when calibrating DAP meters. It is positioned behind the $5 \times 5\,\mathrm{cm}^2$ square aperture which exit is 98 cm the tube focus.
(b) The monitor chamber that can be used for determination of the irradiated time can be positioned here (it is not completely seen in the picture).
(c) The filtration wheel for the different radiation qualities and a lead shutter behind the filtration hole where the radiation comes out. The lead shutter makes it possible to stop the irradiation without turning of the X-ray tube.

2.1.3 Calibration of the detectors

After measuring with the reference pencil chamber, the Radcal pencil chamber and its corresponding electrometer (Model No. 9010, Serial no. 90-1562) were calibrated. The electrometer measured a signal, M_{Radcal}, in the unit of mGy. One could not measure any collected charge or current, but only what the electrometer displayed with this system which was air-Kerma. The Radcal detector system was originally calibrated during fully irradiation assuming it was a point detector. So the value of air-Kerma that the electrometer displayed was valid if it was fully irradiated. If the Radcal pencil chamber as in this case was partly irradiated it needed a correction of the irradiated length. Also it needed to be a correctly determination of the irradiated time to measure the air-Kerma rate. This was determined using the Capintec 30cc PM30 chamber used for the HVL measurements as a monitor chamber behind the Radcal pencil chamber, see Fig. 7. The monitor chamber was connected to a Keithley 35040 electrometer which can give an accurate value of the irradiation time, since it turns on the timing when it detects radiation and turns of the timing when no radiation is detected. The turning on and off for the irradiation was made with the lead shutter seen in Fig. 7. The signal from the Radcal pencil chamber measured in the specific radiation qualities Q, was corrected in the following way to get the air-Kerma rate:

$$\dot{\mathrm{K}}_{Q_{Radcal}} = \frac{M_{Radcal} \cdot k_p \cdot 10}{w} \cdot \frac{1}{t} \qquad [\mathrm{mGy/s}] \tag{7}$$

where M_{Radcal} was the read value from the electrometer in mGy. The term 10 was the effective length of the chamber in cm. k_p, was the correction for temperature and pressure. $w = 5.10$, was the irradiated length in cm according to Eq. 6 and, t, was the irradiation time in seconds received from the monitor chamber. Measurements with the Radcal pencil chamber were performed 3 times during 60 seconds of irradiation. Averaging was made from the three measurements.
The CT Dose profiler (CTDP) can not measure a signal integrated over a length due to its small size of $\sim 250\,\mu$m. Instead it is assumed that the CTDP measures the air-Kerma in a point. The calibration of the CTDP was made with the same physical arrangement as with the pencil chambers, see Fig. 6 - 7. The CTDP with its corresponding measuring system, the Barracuda multimeter (serial no. BC1-08100077) and the software Ocean(Version. 2013.03.18.86), from RTI Electronics, measured the collected charge in a timed mode for 20 seconds repeated three times. Meaning that the system itself stopped measuring after 20 seconds. It also displayed for how long time it had been collecting signals, which could deviate $\pm$ 20 milliseconds. Hence the displayed measuring time was used as the measuring time, t.

The measured air-Kerma rate from the reference pencil chamber, Eq. 5, was used to calculate a calibration factor for the other two detectors.
For the Radcal pencil chamber for each of the radiation qualities, Tab. 2, calibration factors were calculated in the following way:

$$\mathrm{N}_{K,Q} = \frac{\dot{\mathrm{K}}_{Ref,Q}}{\dot{\mathrm{K}}_{Q_{Radcal}}} \qquad [\mathrm{mGy/mGy}] \tag{8}$$

For the CT Dose Profiler calibration factors for each of the radiation qualities Q, Tab. 2, were calculated in the following way:

$$\mathrm{N}_{K,Q} = \frac{\dot{\mathrm{K}}_{Ref,Q}}{\bar{C}_Q/\bar{t}} \qquad [\mathrm{mGy/nC}] \tag{9}$$

Where, $\bar{C}_Q$, was the mean collected charge in the unit of nC in the specific radiation qualities Q, during the mean time $\bar{t}$, displayed from the three measurements.

2.1.4 Normalization

When calibrating detectors used for applications in CT the calibration coefficient is generally normalized to radiation quality RQT 9 [4]. Hence a correction factor, k_Q, is supplied for the other radiation qualities. In this report normalization was also made to radiation quality RQT 9. Radiation quality correction factors[3] dependent for the radiation qualities for the calibrated detectors was calculated in the following way:

$$k_Q = \frac{N_{K,Q}}{N_{K,RQT9}} \tag{10}$$

2.1.5 Uncertatinties during calibration

The uncertainties associated with the calibrations was evaluated according to, 'Guide to the Expression of Uncertainty in Measurement' [11], see Appendix A. For the measurements between the reference pencil chamber (DCT 10) and the Radcal pencil chamber the irradiated length, w, was the same. Hence no extra uncertainties in this regard was taken into account between those two detectors. For the CTDP however the effective irradiated length was not the same, since the diode in the CTDP was assumed to be a point. The irradiated length, w, for the reference pencil chamber was needed according to Eq. 5 to know the air-Kerma to point. For the irradiated length, w, according to Eq. 6, a uniform distribution with an estimated uncertainty of 0.1 cm was taken into account. Which in turn gave an extra uncertainty for the CTDP but not for the Radcal pencil chamber in this regard.

2.2 Evaluating the Mover system

2.2.1 Evaluating the accuracy of measuring the FWHM of beam profiles with the Mover system

In order to measure the $CTDI_{100}$ on a CT scanner the 'dose' profile needs to be integrated over 100 mm. The CTDP can not directly measure over this integration of length since it assumed to be a point-like detector. Instead it is dependent to accurately be moved through this length of irradiation. RTI Electronics have recently released a Mover system that can be used together with the CTDP. This Mover system gives a solution to measure the CTDI when no table translation is possible. The Mover used in this project was a prototype with serial number 001. In Fig. 8 the principle of how the CTDP can be moved with the Mover is shown. A steel wire is threaded to the CTDP and an electrical motor moves the wire. When measuring free in air a PMMA plastic tube is used to give support for the CTDP.
Not only measuring the $CTDI_{100}$ or CTDI along any length of choice is possible with this system. It is also possible to measure the actual full width at half maximum (FWHM). FWHM is often not the same as the nominal collimation determined from the manufacturer of the CT scanner.

[3]Radiation quality correction factor, Beam quality correction factor, Energy correction factor are synonymously used terms. Different sources use different terms. The term, Energy dependence, is often colloquially used and also refers to the same meaning.

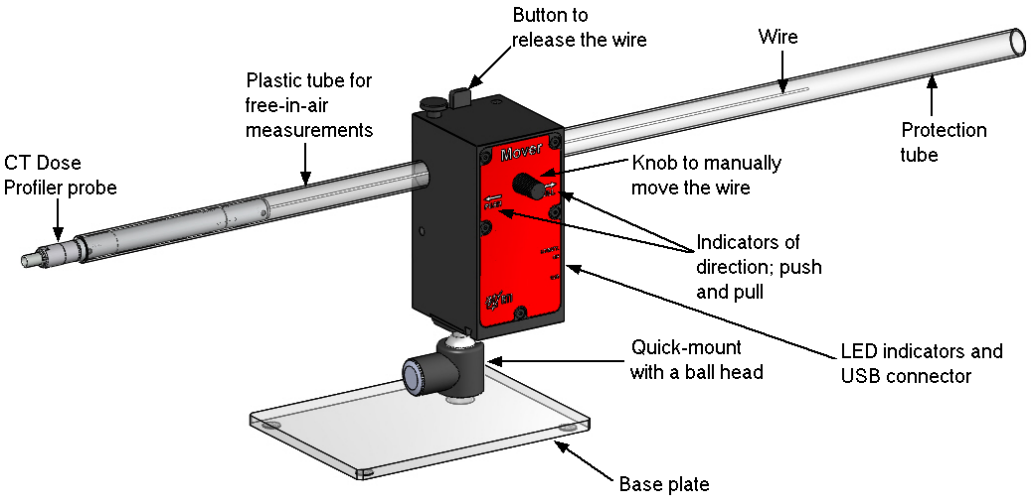

Figure 8: Explanatory picture of how the RTI Mover looks like and the principle of moving it with a steel wire. The plastic tube is necessary to give support for the CTDP when measuring free in air. The picture is reproduced with permission by RTI Electronics:
RTI Electronics. Mover User's Manual - English - Version 1.0C, page 11.

The accuracy of measuring the FWHM with this system was performed at the SSDL. The Mover together with the CTDP, were set up in the same way as when the calibration procedures were made i.e. with the $5 \times 5\,\mathrm{cm}^2$ lead aperture which was exactly 98 cm from the tube focus and the centre of the CTDP placed exactly 100 cm from the tube focus, see Fig. 6. Inside the $5 \times 5\,\mathrm{cm}^2$ opening a lead insert of 2 cm width could be placed to further collimate the beam. In the measuring software Ocean, one can choose with what speed the Mover moves the CTDP. The highest speed being 83.3 mm/s and the lowest 14.9 mm/s and several speeds to choose in between. Measuring was repeated two times in both 50 mm collimation and 20 mm collimation with mover speeds, 83.3, 55.6, 41.7, 27.8 and 18.5 mm/s. But repeated three times with the lowest mover speed 14.9 mm/s. The CTDP total traveling with the Mover was set to be 100 mm in all measurements, letting the travel start and stop well outside the opening of the collimations. The measured FWHM was automatically calculated in Ocean. The measured FWHM was compared to the beam widths, w. The true beam widths was assumed to be described by Eq. 6. Giving $w = 51.0$ and $w = 20.4$ mm respectively for the collimations used.

2.2.2 Evaluate how the plastic tube affects the measured signal with the CTDP

The Mover system has a PMMA plastic tube for the CTDP to give support for it when measuring free in air, see Fig. 8. The wall thickness of the plastic tube was measured to be 1.3 mm. How this plastic tube affects the signal that the CTDP measures was investigated. All the measurements during calibration were made free in air, but also made with the plastic tube on the CTDP. It was studied how the the collected charge was affected due to the plastic tube.

2.3 Testings of the Detectors on Clinical CT-scanners

To see how the calibrated detectors were performing for dosimetric measurements clinically, they were tested on a clinical CT at Sørlandet Hospital in Kristiansand, Norway. See Fig. 9 to get an insight on how the measurements were performed. The CT was a SPECT-CT from GE Healthcare (GE Discovery NM/CT 670) but only the CT system was used (GE Brightspeed Elite 16 Slice CT). Essentially the two calibrated detectors were used, the Radcal pencil chamber and the CTDP. But three different measurements techniques were used. Firstly, helical scanning and measuring with the CTDP. Secondly, axial scanning and measuring with the CTDP that was moved through the irradiation with the Mover. Thirdly, axial scanning and measuring with the Radcal pencil chamber.
Measurements with the detectors were performed free in air, in the conventional Body and Head phantoms, see Fig. 1, and in a specific Pediatric phantom with a diameter of 10 cm. In the pediatric phantom measurements were only performed with the Radcal pencil chamber, since the holes were a bit to small for the CTDP. When measuring in the CTDI phantoms, the phantoms were placed on the patient table. Positioning was made with help from lasers integrated in the CT. When measuring free in air, the different detectors were positioned in the isocentre completely free in air. The plastic tube was on the CTDP for all measurements free in air.
When measuring with the Radcal pencil chamber, measurements were performed in all holes in the phantoms. According to Eq. 3 and 4 the CTDI_w and CTDI_{vol} could then be calculated. The temperature and pressure was noted and the measurements with the Radcal pencil chamber were corrected for that. This correction was not necessary for the CTDP since it is a solid state detector.
When measuring with the CTDP and its corresponding measuring system, the Barracuda multimeter and the software Ocean, measurements were only performed in the central hole in the phantoms. This is explained by that with a pencil chamber, one measures directly the integrated exposure along its effective length. The CTDP is instead measuring the exposure rate from points along a length due to it being moved. In a peripheral hole the measured exposure rate with the CTDP will vary dependent on where the X-ray tube is relative to the CTDP. However, along a length in the central hole the exposure rate will be approximately the same during the whole tube rotation. Hence the CTDP can validly be used for measurements in the central hole, [12]. To get the CTDI_w from measuring with the CTDP one multiplies the CTDI_{100} with a k-factor, that is defined as $\mathrm{k}= \frac{\mathrm{CTDI}_w}{\mathrm{CTDI}_{100}}$ [12], where CTDI_w is originally measured with a pencil chamber.
The scanner parameters that were tested was, tube voltage in kV, nominal collimation and SFOV. When measurements were performed during helical scanning with the CTDP, also different values of pitch were tested. Some of the collimations available for axial scanning were not available for helical scanning, only 10 mm and 20 mm were available for helical scanning. All scanning was made with the same scanning protocol. Also noted for each measurement was the displayed nominal CTDI_{vol} so it could be compared with the measured value. Different SFOV was only tested with the pencil chamber. Different values of pitch during helical scanning with the CTDP was not tested free in air. When measuring free in air with the Radcal pencil chamber, two different values of tube current was used, 100 mA and 300 mA. See Tab. 3 for the measurements made and also the relevant input parameters. Such as tube current in mA, the tube rotation time, t_r, in seconds and mover speed, v_m, in mm/s.

Table 3: The different scanning modes, measurement techniques and phantoms that were used for measuring the $CTDI_{100}$ during different parameter settings on a GE Brightspeed Elite in Kristiansand, Norway. Measurements in the pediatric phantom was only performed with the Radcal pencil chamber. The Radcal pencil chamber was used for measuring in all holes in the phantoms. The CTDP was only used in the central holes. The ***emphasized*** parameters correspond to the reference settings used when another parameter was tested. Over each measuring sequence the relevant input parameters are shown. When one of those input parameters was changed for a specific measurement it is noted with an underbrace.

Scanning mode:	Helical Scanning	Axial Scanning	Axial Scanning
Measurement technique	CT Dose Profiler	CT Dose Profiler with Mover	100 mm Radcal Pencil Chamber
Pediatric phantom ø= 10 cm			**100mA, t_r = 1s** [kV] 80, 100, ***120***, 140 Collimation [mm] 1.25, 5, ***10***, 20 SFOV ***Large***, Small, Head
Free in air	**80mA, t_r = 1s** [kV] 80, 100, ***120***, 140 Collimation [mm] ***10***, 20 SFOV ***Large*** Pitch ***0.625***	**80mA, t_r = 4s** **v_m = 83.3mm/s** [kV] 80, 100, ***120***, 140 Collimation [mm] 1.25, 5, ***10***, 20 SFOV ***Large***	**100mA, t_r = 1s** $\underbrace{80}_{200mA}$, 100, ***120***, 140 $\underbrace{1.25}_{300\&100mA}$, 5, ***10***, 20 SFOV ***Large***, Small, Head
Head phantom ø= 16 cm	**100mA, t_r = 1s** $\underbrace{80}_{200mA}$, 100, ***120***, 140 Collimation [mm] ***10***, 20 SFOV ***Large*** Pitch ***0.625***, 0.875, 1.35, 1.675	**200mA, t_r = 3s** **v_m = 83.3mm/s** [kV] 80, 100, ***120***, 140 Collimation [mm] 1.25, 5, ***10***, 20 SFOV ***Large***	**200mA, t_r = 1s** 80, 100, ***120***, 140 1.25, 5, ***10***, $\underbrace{20}_{150mA}$ SFOV ***Large***, Small, Head
Body phantom ø= 32 cm	**100mA, t_r = 1s** $\underbrace{80, 100, ***120***, 140}_{200mA}$ Collimation [mm] ***10***, 20 SFOV ***Large*** Pitch ***0.625***, 0.875, 1.35, 1.675	**400mA, t_r = 3s** **v_m = 83.3mm/s** [kV] 80, 100, ***120***, $\underbrace{140}_{380mA}$ Collimation [mm] 1.25, 5, ***10***, 20 SFOV ***Large***	**400mA, t_r = 1s** 80, 100, ***120***, $\underbrace{140}_{380mA}$ 1.25, 5, ***10***, 20 SFOV ***Large***, Small, Head

To complement some of the measurements, testings between the CTDP and the Radcal pencil chamber was made on another scanner at Sahlgrenska University Hospital in Gothenburg, Sweden. The scanner used was from GE Healthcare (GE Discovery CT 750HD). The measurements were only performed free in air for different collimations. Different values of pitch during helical scanning with the CTDP was also tested. The FWHM that the CTDP can measure was also noted, to see how the FWHM would be affected for different settings, see Tab. 4. The plastic tube was always on the CTDP for these complementary measurements.

Table 4: The different scanning modes and detector systems that were used for measuring the $CTDI_{100}$, free in air, during different parameter settings on a GE Discovery CT 750HD in Gothenburg, Sweden. The ***emphasized*** parameters correspond for the reference settings that was used when another parameter was tested. Over each measuring sequence the relevant input parameters is shown. When one of those input parameters was changed for a specific measurement it is noted with an underbrace. During helical scanning at 20 mm collimation different values of pitch were also tested. For the CTDP both during helical scanning and axial scanning FWHM was noted.

Scanning mode:	Helical Scanning	Axial Scanning	Axial Scanning
Measurement technique	CT Dose Profiler	CT Dose Profiler with Mover	100 mm Radcal Pencil Chamber
	100mA, t_r = 1s 120kV, Large(SFOV)	**100mA, t_r = 2s, v_m = 83.3mm/s 120kV, Large(SFOV)**	**100mA, t_r = 1s 120kV, Large(SFOV)**
Free in air	Collimation [mm] ***20***, $\underbrace{40}_{pitch=0.516}$	Collimation [mm] 1.25, 5, ***10***, 20, 40	Collimation [mm] $\underbrace{1.25, 2.5}_{t_r=2s}$, 5, ***10***, 20, 40
	Different Pitch tested at Collimation=***20*** mm: ***0.531***, 0.969, 1.375		

The CTDP has integrated energy correction factors that are automatically taken into account when input parameters such as kV, filtration and if measuring is performed in one of the CTDI phantoms or free in air, are specified from the user in the software Ocean. The energy correction factors are normalized to radiation quality RQR 9 IEC 61267:1994. This quality was not used during the calibration procedure. Since this is the reference quality for the CTDP, the measured calibration factor and energy corrections from the calibration procedure was not taken into account for the clinical measurements. Instead the supplied calibration factor from purchase was used, which was $N_k = 0.2655$ mGy/nC in RQR 9 IEC 61267:1994 and calibrated at SWEDAC in 2012-12-10. During all measurements with the CTDP a total filtration of 7 mm Al was specified in Ocean. This was the default setting in Ocean and was not changed.
For the Radcal pencil chamber the performed calibration procedure could be utilized for the clinical measurements. The measured calibration factor from the calibration procedure was used. Some assumptions were made about what energy correction factor should be chosen. For all measurements with the Radcal pencil chamber, it was assumed that RQT 8 simulated most properly when the voltage was 80 kV or 100 kV. RQT 9 was chosen when the voltage was 120 kV and RQT 10 for 140 kV.

From all the measurements, Tab. 3 - 4, comparisons were made between the three different detector systems. From the measurements in the CTDI phantoms, comparison were made on CTDI_{100} measured centrally ($\mathrm{CTDI}_{100,c}$). Since the CTDP not was used for measurements in the peripheral holes in the phantoms. Different tube rotation times, t_r, and tube currents, mA, were chosen in the measurements and hence the CTDI_{100} was normalized to the tube current in mA multiplied with the tube rotation time t_r and divided with a factor of 100, i.e. normalized to the number of 100 mAs.

The Radcal pencil chamber with its electrometer gave a value, M_{Radcal}, that needed to be corrected in the following way to get the CTDI_{100} and normalized to the number of 100 mAs:

$$ {}_n\mathrm{CTDI}_{100_{Radcal}} = \frac{M_{Radcal} \cdot 100 \cdot k_p \cdot \mathrm{k}_Q}{\mathrm{NT}} \cdot \frac{100}{t_r \cdot \mathrm{mA}} \qquad [\mathrm{mGy}/100\,\mathrm{mAs}] \tag{11} $$

where M_{Radcal} was the read air-Kerma value in mGy from the electrometer. The term 100 corrected for the pencil chambers length in mm and NT was the nominal collimation in mm. k_p corrected for the temperature and pressure and k_Q for the energy correction factors used. t_r was the tube rotation time in seconds and 100/mA was the correction for the number of 100 mA.

When measuring during helical scanning with the CTDP the CTDI_{100} normalized to the number of 100 mAs was calculated in the following way:

$$ {}_n\mathrm{CTDI}_{100_{CTDP,helical}} = \left[p \sum_{i=1}^{n} D_i \right] \cdot \frac{100}{t_r \cdot \mathrm{mA}} \qquad [\mathrm{mGy}/100\,\mathrm{mAs}] \tag{12} $$

where the pitch, p, was multiplied with the summation of measured 'dose' from i to n where n was the number of measured samplings within 100 mm. This was how the software Ocean automatically calculated the CTDI_{100} [12]. The normalization to the number of 100 mAs was manually made with the ratio $\frac{100}{t_r \cdot \mathrm{mA}}$.

When measuring with the CTDP and the Mover during axial scanning the CTDI_{100} was automatically calculated using Eq. 13. The normalization was manually made with the ratio $\frac{100}{t_r \cdot \mathrm{mA}}$.

$$ {}_n\mathrm{CTDI}_{100_{CTDP,axial+mover}} = \left[\frac{v_m \cdot t_r}{\mathrm{NT}} \cdot \sum_{i=1}^{n} D_i \right] \cdot \frac{100}{t_r \cdot \mathrm{mA}} \qquad [\mathrm{mGy}/100\,\mathrm{mAs}] \tag{13} $$

Essentially Eq. 13 is the same as Eq. 12 since pitch is defined as $\frac{v_t \cdot t_r}{\mathrm{NT}}$, see Eq. 3, where v_t is the table speed. But now with the difference that no table was moved, instead the detector was moved with the mover speed v_m in mm/s. One can notice from Eq. 13 that the CTDI_{100} normalized to the number of 100 mAs is independent of the tube rotation time, t_r.

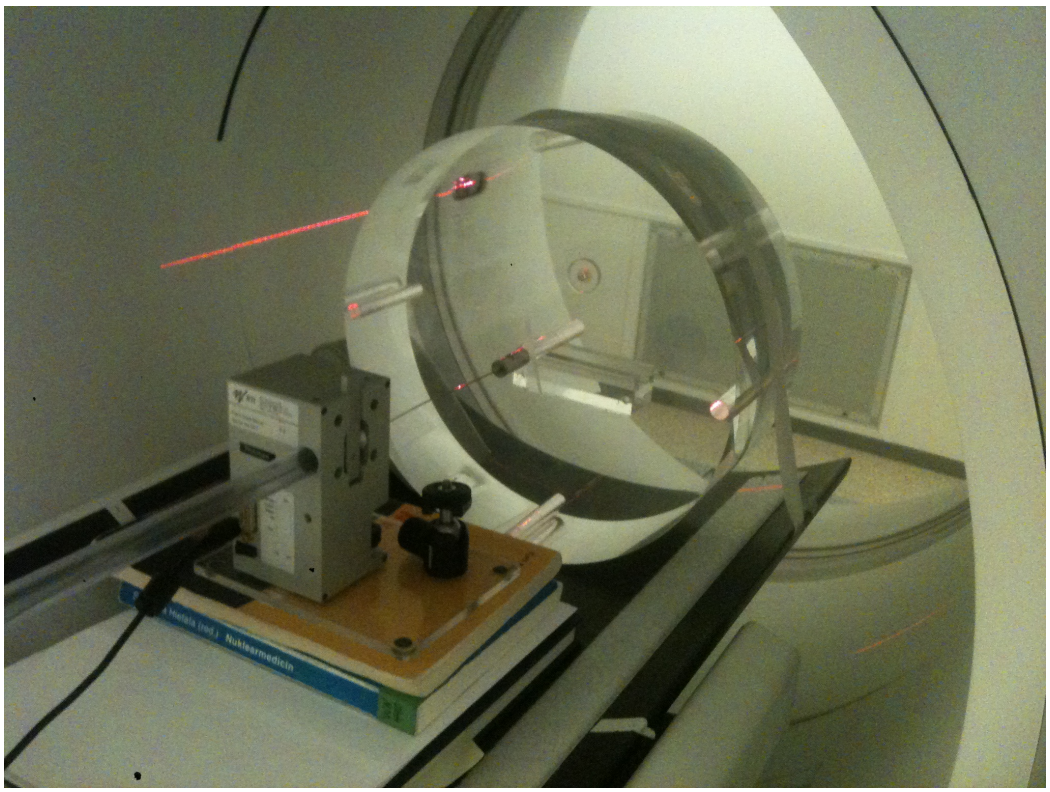

Figure 9: Explanatory picture of how the measurements were performed with the Mover system. This picture demonstrates when the CTDP was used with the Mover during axial scanning in a 32 cm body phantom. The picture is from when the measurements was made using a GE Brighspeed Elite 16 Slice CT in Kristiansand, Norway.

2.4 Evaluate the size dependency of $CTDI_{vol}$ for different phantom sizes

AAPM has recently released a report [6] where four different groups independent of each other, have investigated how $CTDI_{vol}$ can be size converted to other sizes than the conventional CTDI phantoms. A so called size-specific dose estimate (SSDE). Their investigations were made by theoretical Monte Carlo simulations and by practical measurements in different phantoms. With the results they independently achieved and in good agreement between each other, conversion factors for $CTDI_{vol}$ dependent on effective diameter was produced[4]. The term effective diameter is mathematically explained with the following relationship:

$$\text{Effective diameter} = \sqrt{\frac{4 \cdot \text{Area}}{\pi}} \qquad [\text{cm}] \tag{14}$$

and is introduced because patients are not completely round, but can be assumed to be of elliptical shape. Where the lateral width (LAT) and anterior-posterior thickness (AP) in cm are the two parameters that can calculate the effective diameter according to the following relationship:

$$\text{Effective diameter} = \sqrt{\text{AP} \cdot \text{LAT}} \qquad [\text{cm}] \tag{15}$$

The conversion factors, f in AAPM 204 [6], for $CTDI_{vol}$ dependent on effective diameter can be seen in Fig. 10. The conversion factors are valid from knowing $CTDI_{vol}$ for the 32 cm Body phantom or the 16 cm Head phantom.

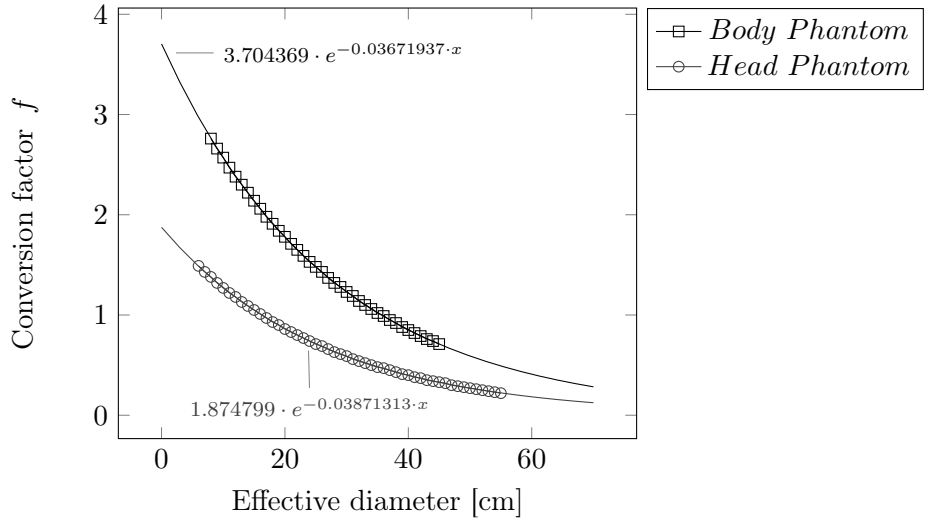

Figure 10: Conversion factors, f, for different effective diameters in cm. The square characters are conversion factors valid for $CTDI_{vol}$ from the 32 cm body phantom. The circular characters are conversion factors valid for $CTDI_{vol}$ from the 16 cm head phantom. The characters are tabulated data reported in AAPM 204 (table 1D & 2D, page 10-11). The lines are best fit exponential trendlines reported in AAPM 204 (page 20).

[4]Conversion factors were not only produced for effective diameters. They were also produced on using the Lateral and/or the Anterior-Posterior dimensions. This project however, only focus on the conversion factors valid for effective diameters.

From knowing two parameters a size-specific dose estimate (SSDE) could be calculated according to the following relationship:

$$\text{SSDE} = \begin{cases} f^{16}_{eff.dia} \cdot \text{CTDI}^{16}_{vol} & \text{CTDI}_{vol} \text{ from Head phantom} \\ \\ f^{32}_{eff.dia} \cdot \text{CTDI}^{32}_{vol} & \text{CTDI}_{vol} \text{ from Body phantom} \end{cases} \quad [\text{mGy}_{(\text{dose})}] \tag{16}$$

where firstly one needed to know the CTDI_{vol}, for one of the two conventional CTDI phantoms, CTDI^{16}_{vol} for the Head phantom or CTDI^{32}_{vol} for the Body phantom. Secondly one needed to obtain a conversion factor, f, shown in Fig. 10. The conversion factor $f^{16}_{eff.dia}$ was valid from CTDI^{16}_{vol} and for a certain effective diameter of the patient. In the same way $f^{32}_{eff.dia}$ was valid from CTDI^{32}_{vol} and for a certain effective diameter of the patient. The SSDE that was calculated according to Eq. 16 was embedded with a dosimetric conversion factor (d-factor) of 1.073 $\text{mGy}_{(\text{dose})}/\text{mGy}_{(\text{air-Kerma})}$. This gave the SSDE in dose to tissue and not air-Kerma.

Measurements of the CTDI_{100} in both the central and peripheral holes were done with the Radcal pencil chamber in the 32 cm body phantom, 16 cm head phantom and in the 10 cm pediatric phantom. This were done with the GE Brigthspeed Elite scanner in Kristiansand, Norway. From these mesurements the CTDI_w according to Eq. 2 and CTDI_{vol} according to Eq. 3 could be calculated for each phantom.

Testing the accuracy of using the size conversion factors, f in Fig. 10, were performed in the following way.
The measured CTDI_{vol} from the 32 cm body phantom and from the 16 cm head phantom respectively was used in Eq. 16 to calculate an SSDE for an effective diameter of 10 cm. The conversion factors, f, that were used was based from the equations seen in Fig. 10, where $x = 10$ in these cases. The conversion factors were divided with the d-factor to consistently get the unit in air-Kerma. The size converted CTDI_{vol} from the head and body phantom to an effective diameter of 10 cm, was compared with the CTDI_{vol} measured in the 10 cm pediatric phantom.

3 Results

3.1 Calibration of Detectors used in CT

Detectors were calibrated in standardized radiation qualities from the reference pencil chamber, IBA DCT 10. Their measured calibration coefficients and energy corrections is shown in Tab. 5. The reference pencil chamber had energy corrections supplied from its calibration certificate from VSL. The CTDP shows the highest energy dependence and the Radcal pencil chamber has a slightly more uniform energy dependence than the reference pencil chamber. Also noted is the estimated measurement uncertainties multiplied with a factor of two (Coverage Factor=2), resulting in a confidence interval of approximately 95% [11].

Table 5: The calibration coefficients, N_k, for the Radcal and CTDP detectors recieved with help from the reference detector, DCT 10, and the expanded measurement uncertainties, U, with a coverage factor= 2. Also noted is the radiation quality correction factors, k_Q, normalized to **RQT 9**. The radiation qualities in this table is based on IEC 61267:2005.

	DCT 10 (The reference) $\mathbf{N_{KL}}$=**26.13** [mGy·cm/nC] U=1.7%	Radcal (Calibrated) $\mathbf{N_K}$=**1.016** [mGy/mGy] U=2.2%	CTDP (Calibrated) $\mathbf{N_K}$=**0.2881** [mGy/nC] U=3.1%
	k_Q From VSL	k_Q measured	k_Q measured
RQT 8	0.958	0.968	0.882
RQT 9	**1**	**1**	**1**
RQT 10	1.083	1.075	1.244
RQR 9	1.026	1.053	1.020

3.2 Evaluating the Mover system

The plastic tube from the Mover system was studied if it had an effect on the signals from the CTDP. The effect was significant and the results are shown in Tab. 6. The greatest effect was seen in radiation quality RQR 9 which has the lowest value of HVL. This effect seems to be dependent on the HVL, Tab. 2.

Table 6: The mean measured collected charge with the CTDP during three exposures of 20 seconds each. From measuring with the CTDP completely free in air or with the plastic tube on. Also shown is the ratio between the measurements in percent.

	Charge [nC] free-in-air	Charge [nC] with plastic tube	Ratio [%] $\frac{\text{with plastic tube}}{\text{free-in-air}}$
RQT 8	19.344	18.135	93.75%
RQT 9	23.888	22.822	95.54%
RQT 10	31.171	30.136	96.68%
RQR 9	51.658	46.645	90.30%

How accurate the FWHM could be measured was investigated for different Mover speeds and the results are shown in Tab. 7. The precision between the measurements seems to be good but a deviation is found for the lowest mover speed, 14.9 mm/s. The accuracy of the measurements are not perfect when the collimations used were known very precisely. The assumed true beam widths, w, from the collimations were calculated according to Eq. 6, and was 51.0 and 20.4 mm respectively. In average when $w = 51.0$ the measured FWHM was 95% of that value. In average when $w = 20.4$ the measured FWHM was 94% of that value.

Table 7: The measured FWHM with the CTDP for different mover speeds during 50 respective 20 mm collimation in the SSDL. The assumed true value of beam width, w, was 51.0 and 20.4 mm respectively for the collimations. This table shows the two measured values of FWHM except for the lowest mover speed 14.9 mm/s where three measurements were made.

Mover speed [mm/s]	Measured FWHM at 50 mm collimation $w = 51.0$ mm [mm]	Measured FWHM at 20 mm collimation $w = 20.4$ mm [mm]
	48.5	19.2
83.3	48.4	19.2
	48.6	19.2
55.6	48.5	19.2
	48.4	19.1
41.7	48.4	19.1
	48.5	19.2
27.8	48.4	19.2
	48.5	19.2
18.5	48.5	19.2
	47.8	18.9
	47.8	19.0
14.9	47.8	19.0

3.3 Testings of the Detectors on Clinical CT-scanners

The FWHM was also measured using a clinical CT scanner. The results are shown in Tab. 8. It can be seen that there is a difference between the measured FWHM and the nominal collimation. It is also seen that the FWHM is always smaller when measuring with the Mover during axial scanning compared to measuring during helical scanning. The measured FWHM seems to be unaffected for different values of pitch. For comparison the FWHM according to the reference manual is shown [14]. Measuring during helical scanning seems to match closer according to the reference manual, than during axial scanning with the Mover. In average the measured FWHM with the Mover was 94% compared to the measured FWHM during a helical scan.

Table 8: The nominal collimations on a GE Discovery 750HD scanner in Gothenburg, Sweden and the measured FWHM. Also noted is the FWHM according to the reference manual. The measurements were made during axial scanning with the CTDP and Mover, with a Mover speed of 83.3 mm/s. Measurements were also made with the CTDP during helical scanning. For helical scanning only 20 and 40 mm collimations were available and for 20 mm collimation different values of pitch were tested. Measured during 120 kV and Large(SFOV).

Nominal Collimation [mm]	Measured FWHM $CTDP_{axial+mover}$ [mm]	Measured FWHM $CTDP_{helical}$ [mm]	FWHM according to reference manual [mm]
1.25	2.7		2.8
5	7.0		7.4
10	12.0		12.4
20	21.0	$\underbrace{22.4}_{p=0.531}$, $\underbrace{22.3}_{p=0.969}$, $\underbrace{22.3}_{1.375}$	21.9
40	40.0	$\underbrace{42.6}_{p=0.516}$	42.2

After the measuring had been done, it was noted that the CT system (GE Brightspeed Elite) chose a larger focal spot when the effect, P=mA·kV, was exceeding 24 kW. The effect from this can clearly be seen in Fig. 16 when measuring with the Radcal pencil chamber. The different curvature for the Body phantom, in Fig. 14, is also due to this larger focal spot.

$CTDI_{100,c}$/100 mAs measured with the different measurement techniques in the phantoms for different tube voltages is seen in Fig. 13 and for different nominal collimations in Fig. 14. A relatively good correspondence is seen, but with a slightly larger difference in Fig. 13 when the tube voltage was 140 kV. In average the CTDP, combined both during helical scanning and axial scanning with the Mover, measured 95% of what the Radcal pencil chamber measured. The estimated standard deviation on this average value of 95% is ±6%.

$CTDI_{100}$/100 mAs measured with the different measurement techniques free in air for different tube voltage is seen in Fig. 15 and for different collimations in Fig. 16 and 17. In Fig. 15 a relatively larger difference is seen when the tube voltage was 140 kV. In Fig. 16 and 17 for the smallest collimation the CTDP measured extra small values compared to the Radcal pencil chamber. During 1.25 mm collimation(small focal spot) in Fig. 16 and in Fig. 17, the CTDP measured 63% and 69% respectively of what the Radcal chamber measured. An unexpected value for the CTDP is also seen in Fig. 16, when measuring during helical scanning at 20 mm collimation it measured approximately the same as the Radcal chamber. Disregarding the more protruding values just noticed, the CTDP measured during axial scanning with the Mover in average 78% of what the pencil chamber measured. Disregarding the same protruding values again, the CTDP measured during helical scanning in average 82% of what the pencil chamber measured. The CTDP during axial scanning free in air with the Mover, measured very consistently 5% less than during helical scanning free in air. This dependence was not seen when measuring in the phantoms.

In the following two pages, 'dose' profiles from the measuring software Ocean are shown.

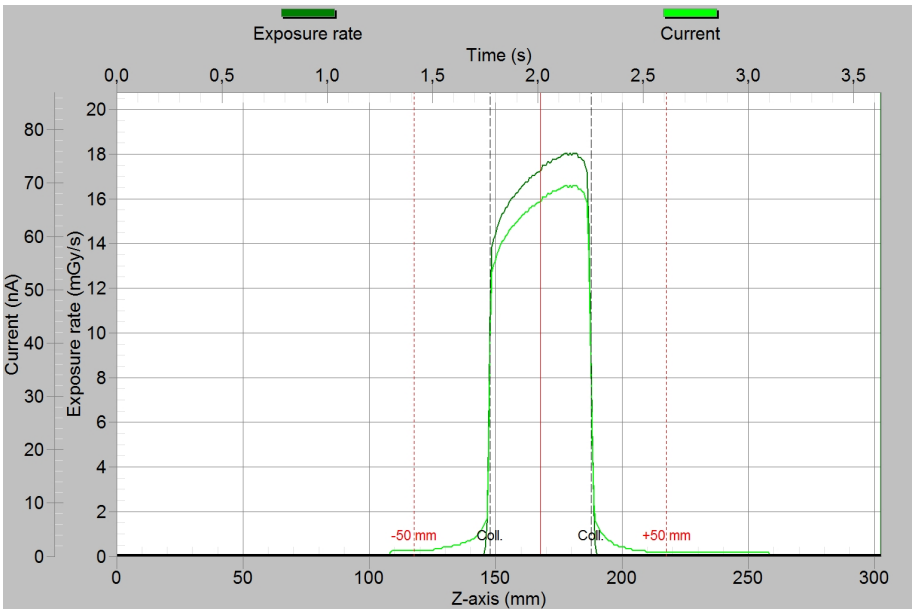

(a)

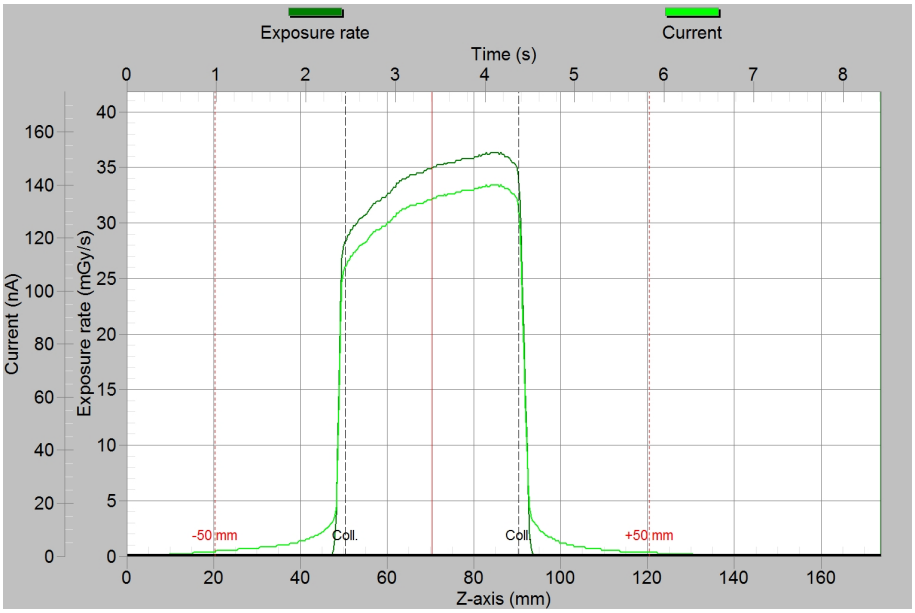

(b)

Figure 11: 'Dose' profiles from the CTDP in the measuring software Ocean when measuring free in air on a GE Discovery 750HD scanner in Gothenburg, Sweden, with 120 kV and Large(SFOV).
(a) 40 mm collimation measured during axial scanning with the Mover with a speed of 83.3 mm/s, the tube current was 100 mA.
(b) 40 mm collimation measured during helical scanning with pitch 0.516, the tube current was 200 mA.
The difference in width between (a) and (b) is due to different preset of measuring times because of the different speeds the CTDP travelled through the beam. Note that the width in the length scale is approximately the same, but not in the time scale between (a) & (b). The Heel effect is evident from the profiles.

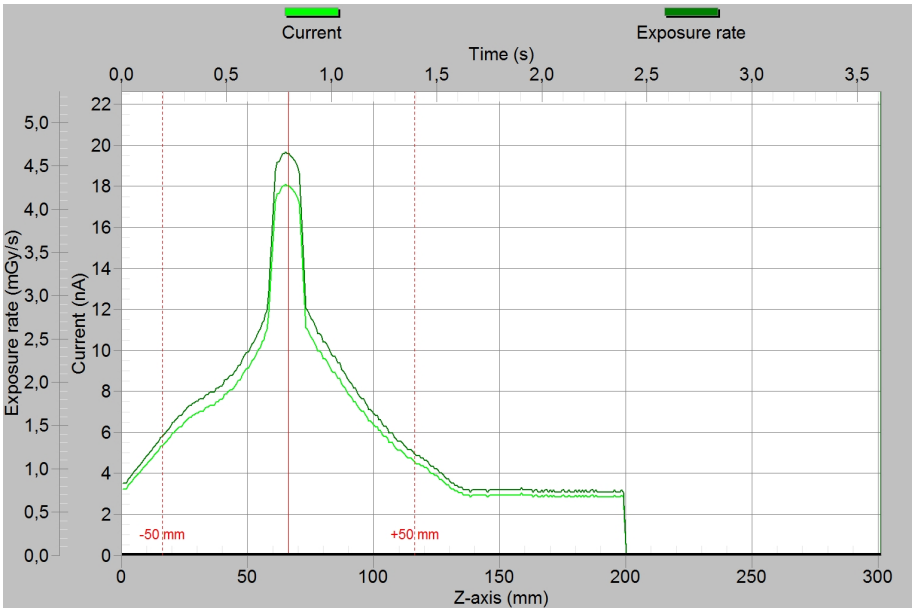

(a)

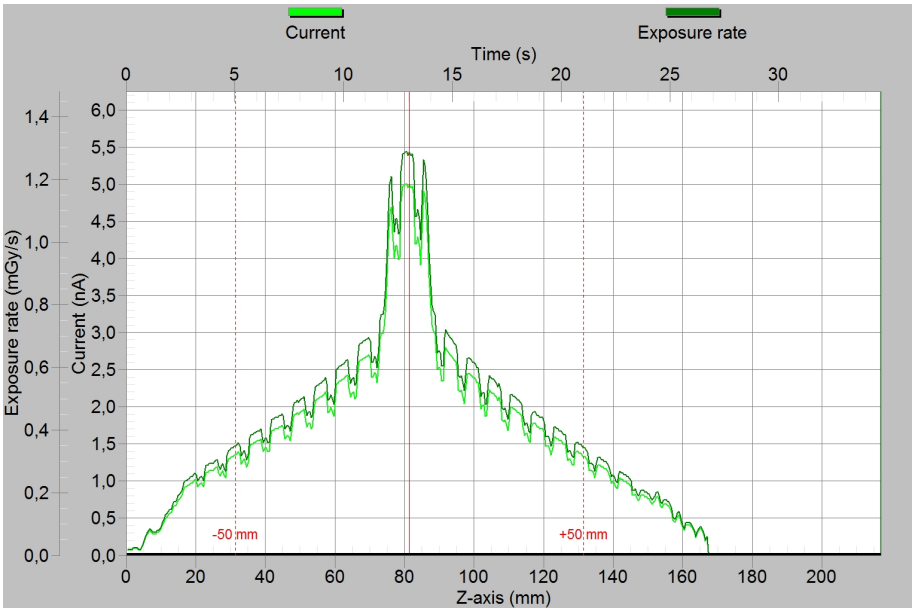

(b)

Figure 12: 'Dose' profiles from the CTDP in the measuring software Ocean when measuring in the Body phantom on a GE Brightspeed Elite scanner in Kristiansand, Norway, with 120 kV and Large(SFOV).
(a) 10 mm collimation measured during axial scanning with the mover with a speed of 83.3 mm/s, the tube current was 400 mA.
(b) 10 mm collimation measured during helical scanning with a pitch of 0.625, the tube current was 100 mA.
The effect from table attenuation is evident from the 'dose' profile in (b). But not in (a) since the tube rotation were slowed down to 3 seconds and the Mover system with the CTDP in this case had time to capture the 'dose' profile while the X-ray tube where above the patient table.

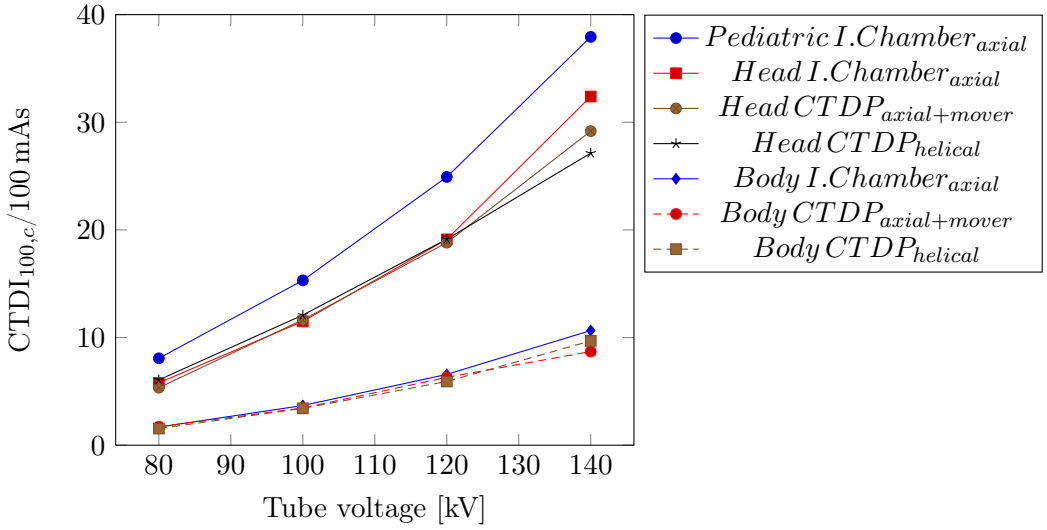

Figure 13: $\mathrm{CTDI}_{100,c}/100\,\mathrm{mAs}$ vs different tube voltages measured in the different phantoms and different measurement techniques. The measurements were made on a GE Brightspeed Elite scanner in Kristiansand, Norway, with Large(SFOV) and 10 mm collimation and with a pitch of 0.625 during the helical measurements. In the pediatric phantom measurements were only made with the Radcal pencil ionization chamber.

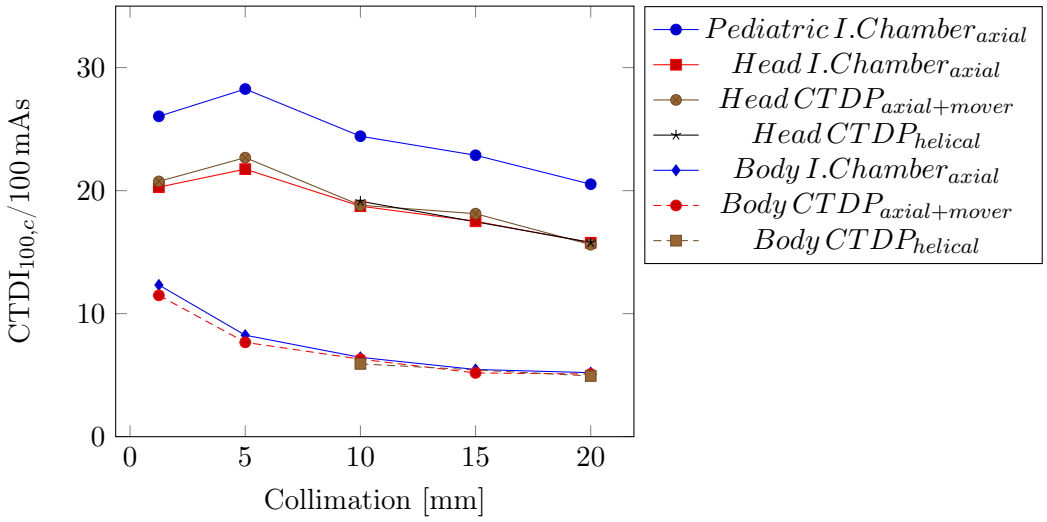

Figure 14: $\mathrm{CTDI}_{100,c}/100\,\mathrm{mAs}$ vs different nominal collimations measured in the different phantoms with the different measurement techniques. The measurements were made on a GE Brightspeed Elite scanner in Kristiansand, Norway, with Large(SFOV) and 120 kV. In the Pediatric phantom measurements were only made with the Radcal pencil ionization chamber. During helical scanning only 10 and 20 mm collimation were available and the pitch was 0.625. The different curvature for the Body phantom is due to the larger focal spot (tube current=400 mA). In the other two phantoms only the small focal was used.

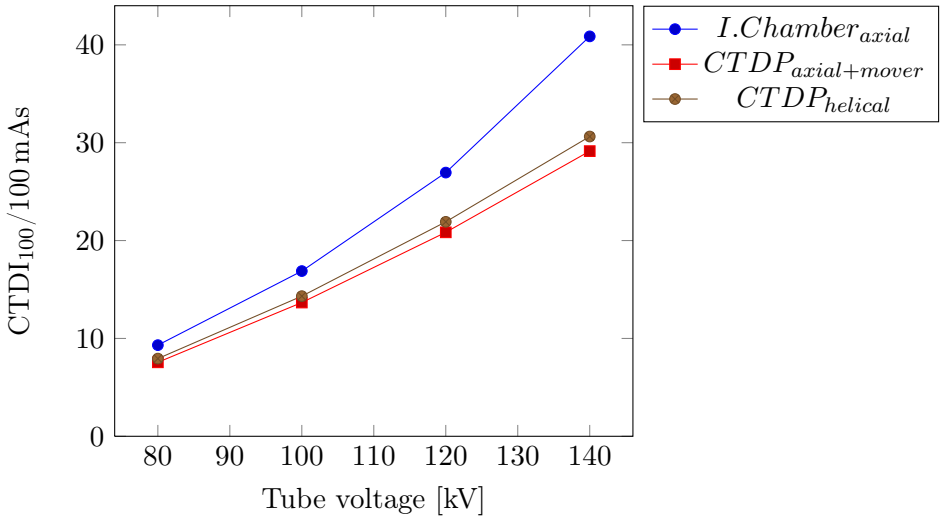

Figure 15: $CTDI_{100}/100\,mAs$ vs different kV measured free in air with the different measurement techniques. The measurements were made on a GE Brightspeed Elite scanner in Kristiansand, Norway, with Large(SFOV) and 10 mm collimation and with a pitch of 0.625 during the helical measurements.

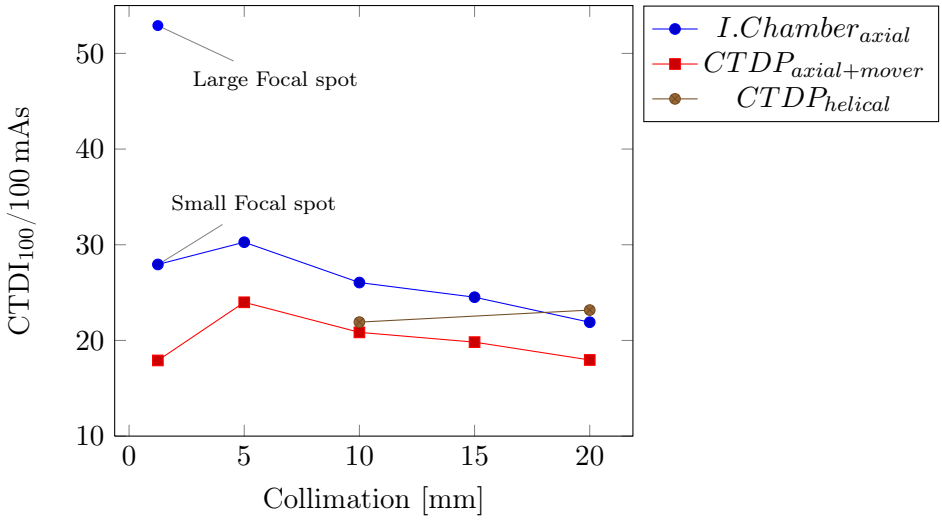

Figure 16: $CTDI_{100}/100\,mAs$ vs different collimations measured free in air with the different measurement techniques. For the smallest collimation (1.25 mm) measurements with the Radcal chamber, were made either with a small focal spot (tube current=100 mA) or a large focal spot (tube current=300 mA). All other measurements referred to in this figure, were made with a small focal spot. The measurements were made on a GE Brightspeed Elite scanner in Kristiansand, Norway, with Large(SFOV) and 120 kV. During helical scanning only 10 and 20 mm collimation were available and the pitch was 0.625.

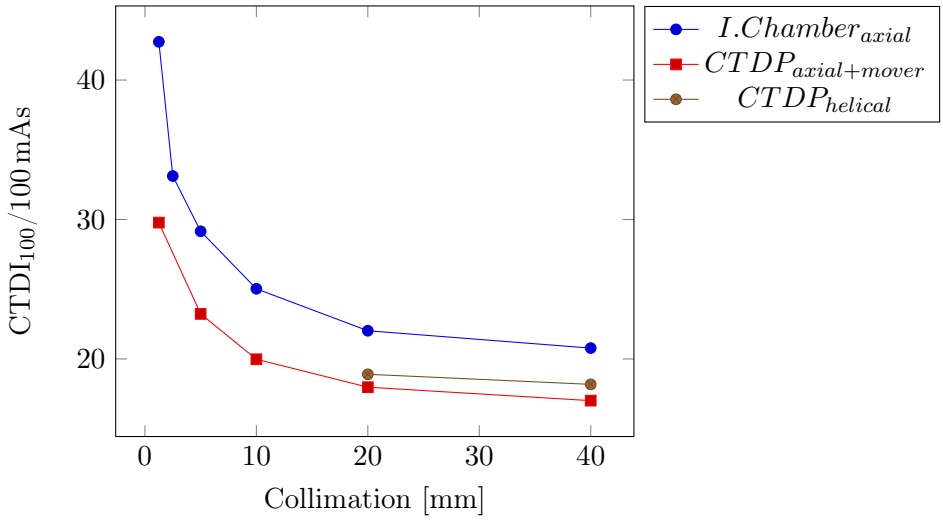

Figure 17: $CTDI_{100}$/100 mAs vs different nominal collimations measured free in air with the different measuring techniques. The measurements were made on a GE Discovery 750HD scanner in Gothenburg, Sweden, with Large(SFOV) and 120 kV. During helical scanning only 20 and 40 mm collimation were available and the pitch were 0.531 and 0516 respectively for the collimations.

In Fig. 18 it can be seen that different values of pitch not have any great effect on the $CTDI_{100}$. Different pitch measured in the phantoms were made on a GE Brightspeed Elite in Kristiansand, Norway. Different pitch measured free in air were made on a GE Discovery 750HD in Gothenburg, Sweden. Also note in Fig. 18 that the collimations are not the same, in the phantoms it was 10 mm and free in air it was 20 mm.

3.4 Evaluate the size dependency of CTDIvol for different phantom sizes

In Fig. 19 it can be seen that the size corrected $CTDI_{vol}$ from the Head and Body phantom was quite near the measured values in the 10 cm Pediatric phantom. Especially for lower kV and larger collimations. A protruding value is seen from the body phantom in the lowest collimation (1.25 mm). When SFOV is Small or Head the measured $CTDI_{vol}$ in the 10 cm Pediatric phantom, is a bit higher than the size corrected values. Before any size corrections were made, the measured $CTDI_{vol}$ for the Head and Body phantom were 84% and 42% respectively of the size corrected value.

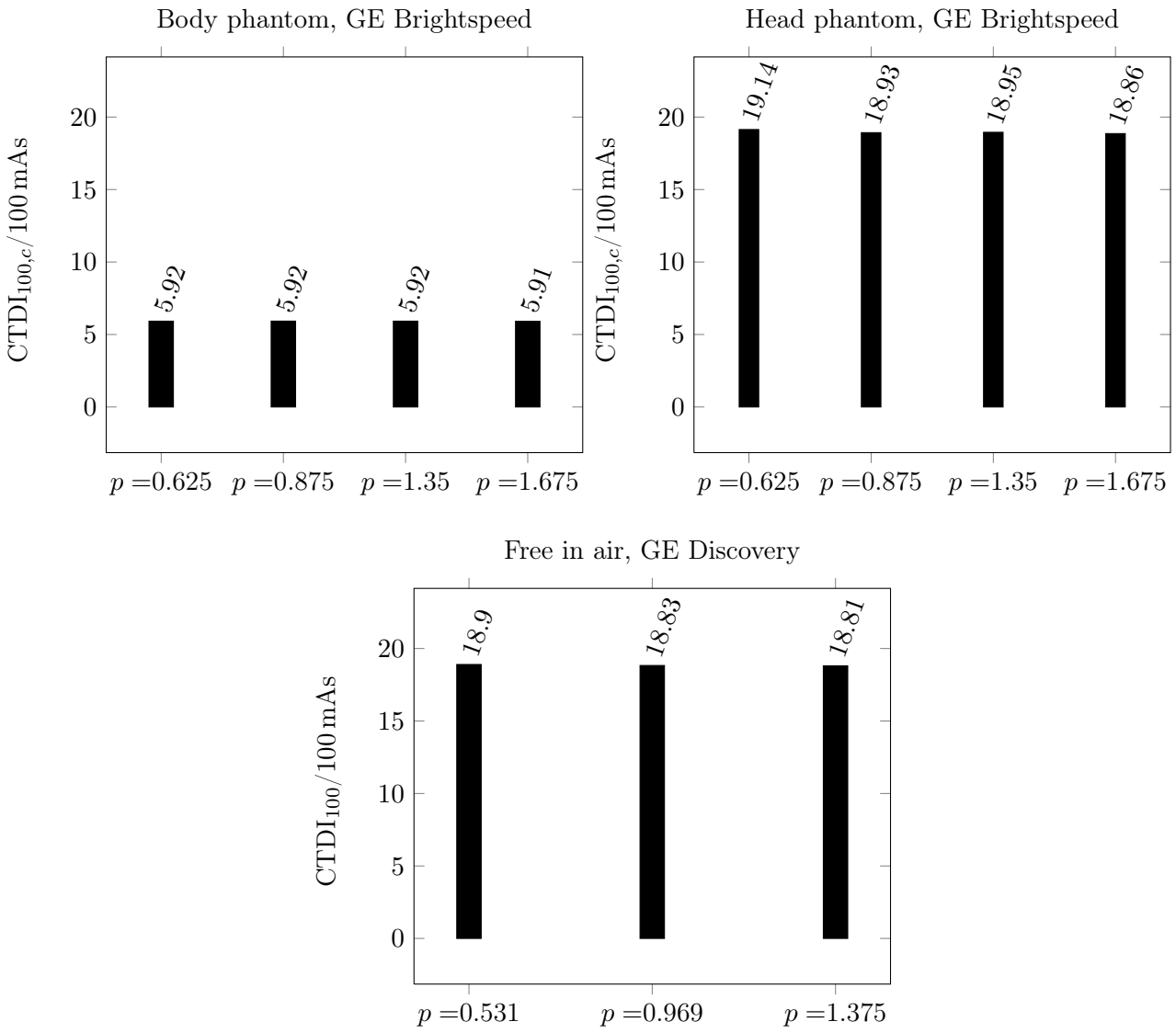

Figure 18: $CTDI_{100}/100\,mAs$ measured with the CTDP during helical scanning with different values of pitch, p, in the different phantoms and free in air. The measurements in the phantoms were made on a GE Brightspeed Elite scanner in Kristiansand, Norway and free in air on a GE Discovery 750HD scanner in Gothenburg, Sweden. The values of pitch differed between those scanners. The measurements were made with 120 kV and Large(SFOV). In the phantoms the collimation was 10 mm and free in air it was 20 mm.

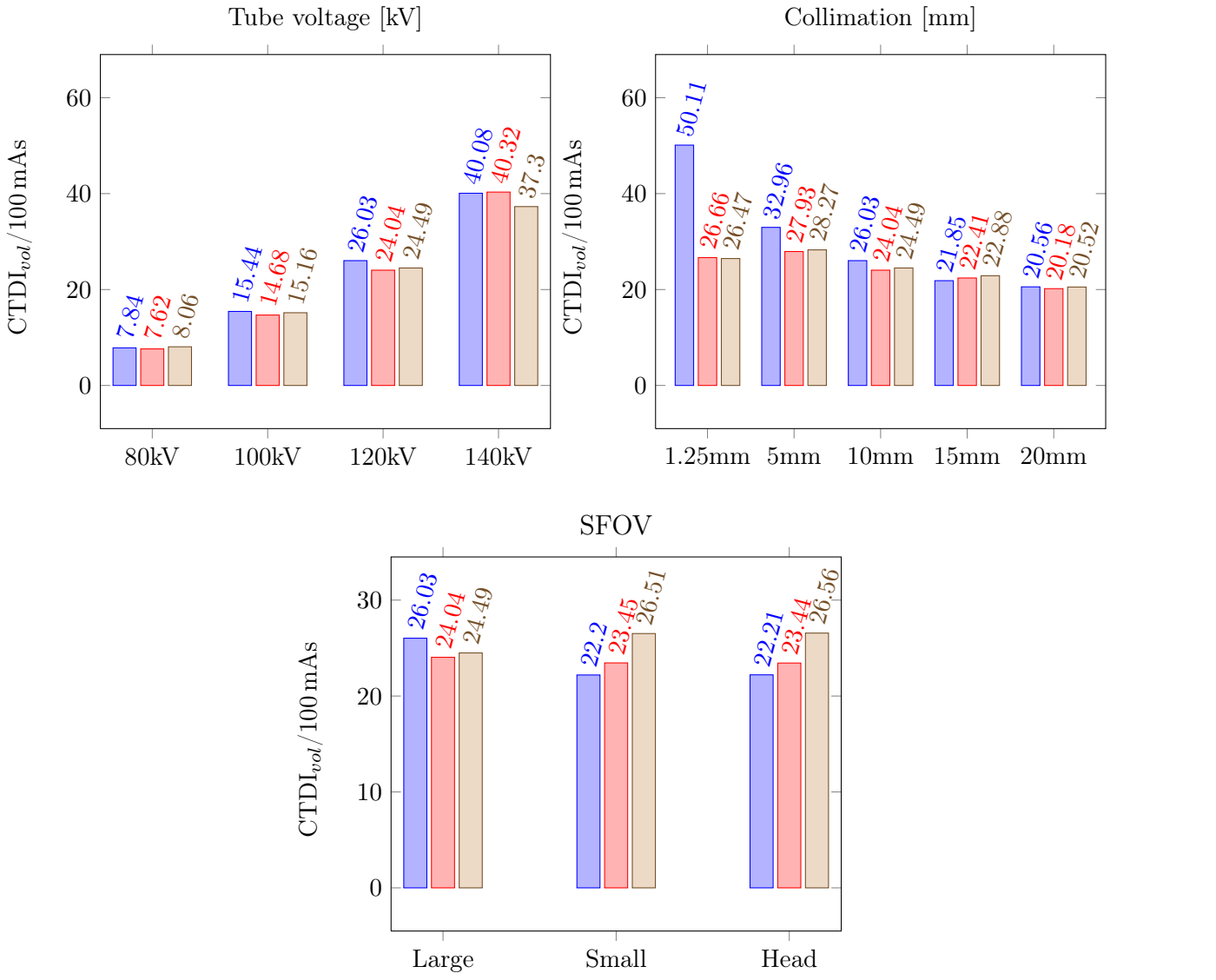

Figure 19: CTDI$_{vol}$/100 mAs size corrected from the 32 cm body phantom and the 16 cm head phantom respectively to an effective diameter of 10 cm and the measured CTDI$_{vol}$ in the 10 cm pediatric phantom. The data is shown when either tube voltage, collimation or SFOV was the parameter of change and was measured with the Radcal pencil ionization chamber during axial scanning. The measurements were made on a GE Brightspeed Elite scanner in Kristiansand, Norway. Large(SFOV), 10 mm collimation and 120 kV were the reference settings when another parameter was tested.

4 Discussion

4.1 Calibration of Detectors used in CT

Three detectors were used for calibration measurements, one of which was the reference pencil chamber (IBA DCT 10). The two detectors that were calibrated and the reference pencil chamber all handled the signal of response in a different way. The reference pencil chamber was originally calibrated during partial irradiation, a similar procedure that was established during this project and in a manner as described by IAEA 457 [4]. However the Radcal pencil chamber was originally calibrated during fully irradiation then assuming it was a point detector that together with its corresponding electrometer was set to give a value in mGy. This was why the Radcal pencil chamber during partial irradiation needed a correction for the irradiated length and also got the calibration factor in the unit of mGy/mGy, Tab. 5. Lastly the CTDP do not share two of the physical attributes that the ion chambers have. The radiation interacts in a solid material instead of a gas and the signal is not created along a length. To be able to calibrate the CTDP from a reference pencil ionization chamber, some extra considerations about the irradiated length needed to be made. This gave an extra uncertainty to the calibrated CTDP. In Tab. 5 it shows that the CTDP has the biggest energy dependence. It also shows that the energy dependence for the reference pencil chamber is a bit higher than the calibrated Radcal pencil chambers energy dependence. It should also be noted, that from a calibrating point of view although all parameters are kept under control to that extent that is possible for a SSDL. Using a reference chamber that has the relative high energy dependence as in this project, is not ideal.

4.1.1 Establishing a calibration procedure for detectors used in CT

In this project a calibration procedure was established. It was based on two references, firstly and foremostly, in a manner on how the reference pencil chamber was originally calibrated. But also as described by IAEA 457 [4]. The established calibration procedure in this project is highly valid for the current dosimetric paradigm in CT where the pencil ionization chamber is indispensable. But it is also a quite circumstantial calibration procedure, meaning that it is easy to make errors. However the established procedure also works for calibrating point-like detectors. But it should be noted that it introduces greater uncertainties for these kind of detectors due to the irradiated length that must be used to get the reference air-Kerma. To calculate the irradiated length, as is done in this project, is not the most credible way to handle the length of irradiation. Film dosimetry is a possible way to handle this instead, however it is not straightforward and in the end not as accurate as one could wish for. Remember that it is irradiation lengths of tenths of a millimeter that needs to determined.
As is described in the introduction, the current dosimetric paradigm in CT is loosing its validity. A new dosimetric paradigm is starting to be established, [8, 13]. This paradigm based on using point-like detectors instead. Since the whole dosimetry for CT is seemingly starting to be restructured in a way where it is valid for any beam width. Perhaps also the calibration procedures, which has a highly significant part in the dosimetry, needs to be restructured. This new calibration procedure, simply based on knowing the air-Kerma to a point with for example using a Farmer chamber. The faithful Farmer chamber can in a PSDL be calibrated for air-Kerma to knowing its accuracy within $\sim 4‰$. A much higher degree of certainty than for example the reference pencil chamber used in this project, Tab. 5. Calibration of pencil ionization chambers would still be valid with this procedure if they were

fully irradiated. Then assuming they also are point-like detectors. Some of the contributing factors of uncertainty would then be how homogenous the radiation field is for the pencil chamber. Also the stem effect and differences in ion collecting potential near the ends of the central electrode would contribute. It should be investigated with how large uncertainties these factors would contribute.
Lastly one question that should be asked but not answered here, is the question if not the whole dosimetry in CT should be restructured to knowing the absorbed dose to water instead.

4.2 Evaluating the Mover system

4.2.1 Evaluate how the plastic tube affects the measured signal with the CTDP

In Tab. 6 it shows that using the plastic tube when measuring free in air affects the measured signal for the CTDP. A rough estimate on radiation quality RQT 8 with 100 kV, assuming a mean energy of $\frac{2}{3} \cdot 100 \sim 60$ keV and a wall thickness of 1.3 mm PMMA with attenuation coefficients received from NIST [16], the estimated attenuation due to the PMMA will be $\sim 3\%$. This meaning that the measured differences shown in Tab. 6 can not be fully explained with just the attenuation from the plastic tube. As is shown in Tab. 5 the energy dependency for the CTDP is relatively high. Possibly the plastic tube differs the radiation quality that the diode in the CTDP is measuring and hence the difference maybe is explained.
When measuring with the CTDP and the Mover free in air with the plastic tube on, perhaps it could need radiation quality factors specific for when the plastic tube is on, or finding another solution on how to move the CTDP without a plastic tube.

4.2.2 Measuring the FWHM

When measuring the FWHM with the Mover in the SSDL the values seemed to be consistent for all speeds except the lowest one, 14.9 mm/s. In this thesis the assumption is made that the true width of the collimated beam is explained by Eq. 6. According to this assumption the true widths of the beam should be 51.0 and 20.4 mm and the measured FWHM with the Mover system was approximately 48.5 and 19.2 mm respectively, Tab. 7. The system showed a good precision between measurements but the accuracy of it needs to be investigated further. A possible source of error is the accuracy of the Mover speed, since it affects the time it is in the beam and further on the calculation of the FWHM.
When measuring the FWHM on a clinical scanner, Tab. 8, there was a difference between the nominal collimation and the measured FWHM. This was also expected since the nominal collimation displayed from the scanner not equals the actual FWHM in the rotation centre. This was also substantiated from to the values in the reference manual. The nominal collimation actually corresponds to an image parameter and not the physical beam width [8]. The measured FWHM from the Mover was slightly below what the reference manual said. The measured FWHM from helical scanning was slightly above but more close to what the reference manual said. This could point to that the scanner collimation was affected whether it was in axial or helical scanning mode. The values from the reference manual was measured during helical scanning. However it is interesting to point out that when measuring with the Mover, it always measured $\sim 95\%$ of what was expected. Both in the SSDL Tab. 7 and compared with the measured FWHM during helical scanning, Tab. 8. This probably means that the Mover speeds are slightly higher than what is stated. This also points to that the collimation on the scanner was unaffected whether it was in helical or axial scanning mode.

To be able to measure FWHM on a clinical scanner to an accuracy that deserves justification instead of using the nominal collimation, the accuracy of the measuring system should be known. Measuring the FWHM with the CTDP during helical scanning seems to be accurate enough. However when measuring during axial scanning with the Mover the accuracy is dependent on how true the Mover speed is. In conclusion it can be said that when using the Mover system, the Mover itself could need a specific speed calibration or a correction factor in the measuring software Ocean. Also the many Mover speeds that can be chosen is not necessary, two or three accurate Mover speeds should be enough.

4.3 Testings of the Detectors on Clinical CT-scanners

CTDP needs another theoretical approach than measuring with the pencil chamber. Looking at Fig. 11 - 12, what is displayed is how the exposure rate varies for different times. From knowing the speed then the positions can be determined. It is easy to deceive oneself, that it is an exposure profile displaying the exposure for different positions. If one would for example measure the exposure profile with TLD detectors then this approach would be true. But when measuring with the CTDP this approach needs to be changed. For example holding the tube voltage and collimation constant but doubling the tube current and traveling speed, one will measure the same total exposure.
As can be seen in Eq. 13 it was shown that $\mathrm{CTDI}_{100}/100\,\mathrm{mAs}$ was independent of the tube rotation time, t_r. This is not entirely intuitive, but can be explained by the following thought experiment. Assume that the dose to a point somewhere along the rotational symmetry axis, z, is measured with two different point-like detectors. The first detector measures the accumulated dose from a tube rotation, $\mathrm{D}_1(z)$. The second measures the dose rate, $\dot{\mathrm{D}}_2(z)$, during the tube rotation. The following relationship can then be seen between the two detectors :

$$\mathrm{D}_1(z) = \dot{\mathrm{D}}_2(z) \cdot t_r \underbrace{\longrightarrow}_{\text{per mAs}} \frac{\mathrm{D}_1(z)}{\mathrm{mA} \cdot t_r} = \frac{\dot{\mathrm{D}}_2(z)}{\mathrm{mA}} \tag{17}$$

The CTDP measures an exposure rate, hence the tube rotation time, t_r, is cancelled out when CTDI_{100} is normalized to the number of mAs. The pencil chamber measures an exposure. It should be noted that the relationship seen in Eq. 17 is just valid, when the exposure rate is independent of the X-ray tubes position during the rotation. This is why the CTDP not should be measured in the peripheral holes in the phantoms. This approach that needs to be adopted when measuring with the CTDP also explains why the summation of dose values along 100 mm, Eq. 12, needs to be multiplied with the pitch. Or simulated 'pitch' that the Mover system effectively makes, Eq. 13. A clear derivation for this pitch dependence has been shown before [15].

It should be noted that the energy correction factors, RQT 8-10 in Tab. 5, that were used for the Radcal pencil chamber, not perfectly simulate the radiation qualities arising either in the phantoms or when the tube voltage was lower than 100 kV. Also should be noted, that when the tube voltage was 140 kV during clinical measurements, the energy correction factor valid for RQT 10 was chosen for the Radcal pencil chamber and a relatively higher difference compared to the CTDP was seen. If the energy correction factors used for the Radcal pencil chamber were properly chosen is not further investigated in this project. Although, this is one factor that would be interesting to investigate further.

Comparing the CTDP with the Radcal pencil chamber when measuring $CTDI_{100,c}$ inside the phantoms, the consistency was relatively good, Fig. 13 - 14. In average the CTDP measured 95% of what the Radcal measured. Any differences between measuring helically or axially with the Mover was not seen. This should be recognized as a relatively good consistency, especially in that regard that so many input parameters were changed for the different measurement techniques, Tab. 3 - 4. This is also one factor that could have improved this project, in keeping the input parameters more consistent between the measurements. For example after the measurements were made, it was noticed that the system changed to a bigger focal spot when the effect was exceeding 24 kW. This change of size in focal spot gave the greatest affect on small collimations and can be seen in Fig. 14 where the difference in curvature from the body phantom, is explained by this and in Fig. 16 where a great difference was seen when measuring free in air. The good correspondence that was seen when measuring in the phantoms also indirectly points to that the integrated energy corrections for the CTDP are valid.

It is important to keep in mind, that attenuation from the patient table can affect the result (the 'table effect'). Looking at Fig. 12(b) it can be seen how the table attenuates the irradiation during helical scanning. This is not a major problem when measuring during helical scanning for larger collimations. Since the 'dose' profile is 'evened out' due to the relative small positional change for one tube rotation. The lower the pitch will be in this regard, the more it it will be 'evened out'. For smaller collimations however it can affect the results more. The patient table can reduce the measured maximum exposure rate in the centre of the beam relatively more for smaller collimations.
With the Mover measurements were dependent on a single tube rotation, hence the tube rotation was slowed down for these measurements. As just described for helical scanning, analogously, the maximum exposure rate can be reduced if the tube is under the table at same the time when the CTDP is in the isocenter of the X-ray tubes rotational symmetry axis, i.e. in the centre of the beam. This leading to a diminished value of the total exposure. However with that said for example looking in Fig. 18, different values of pitch did not have any great affect on the measured $CTDI_{100,c}$. If the collimation would be very narrow and measuring with the highest pitch, this 'table effect' diminishing the $CTDI_{100,c}$ would probably have occurred between different scanning. Positioning the phantom free in air would solve this problem and has been done before [15].
The 'table effect' is not relevant in the same way for the Radcal pencil chamber since it always measures along a length independently of where the tube is and also during the whole tube rotation. However this 'table effect' is something to be aware of when measuring with the CTDP.
It should also be said that even though the Radcal pencil chamber was reliable for measuring the $CTDI_{100}$ it will always have that great disadvantage that it can not measure for longer lengths than 100 mm. The CTDP do not have this disadvantage and better yet, one can see how much of the 'dose' profile that is captured. Also, the CTDP is not limited to measure the $CTDI_{100}$, measuring the CTDI along any length of choice is possible with this system.

When measuring free in air, Fig. 15 - 17, the consistency was not so good anymore. The assumption was made that the measurements with the Radcal pencil chamber was closest to the truth. The difference seen with the CTDP can possibly partially be explained by that the plastic tube was always on the CTDP both during helical scanning and during axial scanning

with the Mover. The reason for this was that this effect had not been recognized when the measurements were performed. However looking at Tab. 6 the maximum decrease in signal due to the plastic tube was $\sim 10\%$ in RQR 9. In average the CTDP measured 80% compared to the Radcal pencil chamber. So logically it is not just the effect from the plastic tube that is seen. What else that is contributing to this effect needs to be investigated further. It would be very interesting to measure the $CTDI_{100}$ free in air without the plastic tube and see the results.
Comparing the results in Fig. 16 to Fig. 17 a different curvature for different collimations is seen. The reason for this is explained by that it was two different scanners. The results between Fig. 16 and Fig. 17 should for that reason not directly be compared with each other.

Another thing to point out is that when the collimation was very narrow (1.25 mm), the CTDP measured even lower values than the Radcal pencil chamber ($\sim 65\%$). But this effect has been recognized before [12], and is originated from that the diode in the CTDP needs a scattering contribution from wider fields. When the fields are more narrow than 4 cm this effect is automatically corrected for. However there is no valid correction for field sizes as narrow as 1.25 mm, it just goes down to 3 mm. This scattering contribution is not a problem when measuring in the CTDI phantoms since the scattering then is so considerable.

A small difference was also seen when measuring free in air, Fig. 15 - 17, between measuring during helical scanning or with the Mover during axial scanning. Measuring with the Mover during axial scanning the measurements were a bit lower. As is described earlier from the FWHM measurements, it is possible that the actual Mover speed was a bit higher than stated. It is very interesting to point out, that the measurement of the FWHM with the Mover was $\sim 5\%$ lower than the 'true' beam widths, both clinically and in the SSDL, Tab. 7 - 8. When measuring during axial scanning with the Mover free in air, it also consistently measured a $CTDI_{100} \sim 5\%$ lower compared when measuring during helical scanning, Fig. 15 - 17. This possibly states that the Mover speed is $\sim 5\%$ too high. Note that this difference in $CTDI_{100,c}$ was not seen when measuring in the phantoms. Possibly because when measuring in the phantoms the whole exposure profile is not within 100 mm.

In Fig. 16 for 20 mm collimation a protruding value was seen during helical measurement with the CTDP. It gave approximately the same value as the Radcal pencil chamber which was not expected because of the deviation seen for the other measurements. The reason for this is not exactly known. Hence this result should be looked with some oversight.

4.4 Evaluate the size dependency of CTDIvol for different phantom sizes

Fig. 19 shows that the measurements made in the 10 cm phantom compared relatively well with the size corrected measurements made in the 16 cm and 32 cm phantoms. Especially with lower tube voltage and larger collimation. The measured $CTDI_{vol}$ was originally $\sim 80\%$ and $\sim 40\%$ of the size corrected value for the head phantom and body phantom respectively. This says how much $CTDI_{vol}$ can underestimate the exposure for small patients, such as children. A protruding value is seen from the measurement made in the 32 cm phantom during 1.25 cm collimation. A likely explanation for this can be seen in Fig. 14 together with Fig. 16, that the $CTDI_{100,c}$ for the 32 cm phantom do not follow the same curvature as the 16 cm or 10 cm

phantom. This is due to the larger focal spot the CT system automatically chose when the effect was exceeding 24 kW, which was the case actually for all the measurements made in the 32 cm phantom. This highlights that for small collimations it is important to know what focal spot is chosen during the scanning if conversion factors like in this project will eventually be used in the clinic. Actually the larger focal spot was also chosen when the tube voltage was 140 kV in the 16 cm phantom. Highlighting again how this project could have been performed better. But with this in mind, the size-specific dose estimates was quite reliably matching the measured $CTDI_{vol}$ in the 10 cm phantom, with the big exception when the collimation was very narrow with a large focal spot.
The Small SFOV and Head SFOV was using the same bow-tie filter. Hence the measurements gave nearly the exact same $CTDI_{vol}$. However looking into when these SFOV were used during measurements, the size converted $CTDI_{vol}$ from the phantoms were consistently underestimating the measured $CTDI_{vol}$ in the 10 cm phantom. This can perhaps be explained by with using this bow-tie filter, the exposure rate becomes lower the more peripheral from the isocenter one measures. Remember $CTDI_{vol}$ is determined by $\frac{2}{3}$ of the peripheral exposure, Eq. 2. But if this is correct needs to be investigated further.
According to AAPM 204 [6], using this method to correct for size is related with an approximate uncertainty of 20%. But the measurements in this project point to an accuracy greater than that. With that said, the correction factors are tended to be used from the $CTDI_{vol}$ displayed from the scanner console. In this project although not given in the section of results, the $CTDI_{vol}$ displayed from the scanner console was always higher than measured and in average 8% higher. Also this investigation was made during ideal conditions i.e. the pediatric phantom used do not correctly simulate a small real patient. With this in mind, using the size-specific dose estimates from the scanner console to estimate the real patients dose, an uncertainty of 20% as stated is probably reasonable.
It should be noted, that these size-specific dose estimates are directed to be used from $CTDI_{vol}$. They do not solve the propriety in using this parameter. However $CTDI_{vol}$ is so far conventionally used. So with respect for justification and optimization when scanning patients and especially children, size-specific dose estimates should be introduced clinically so that the radiographer and doctor knows the patients estimated dose to a higher accuracy than what is based on a standardized phantom.

5 Conclusion

This project can be structured in four parts. Firstly it focused on calibration procedures for detectors in CT. The calibration procedure that was established was highly valid for pencil ionization chambers and worked for a point-like detector. However, it seems that the dosimetry in CT will enter a new paradigm that will be consistent and robust for any type of CT scanner and beam width. A dosimetry based on using point-like detectors instead. The established calibration procedure turned out to highlight one very important aspect, namely the length of irradiation. This parameter is not as easily handled as one could think. Perhaps calibration procedures in CT should be based on another more simple method. A method of just knowing the air-Kerma to a point.
Secondly the recently released Mover system from RTI Electronics AB was evaluated. The Mover is developed to be used with a solid state point-like detector called CT Dose Profiler (CTDP). When measuring the FWHM with the Mover system it seemed to measure a bit too small lengths. Possibly it travels to fast. However it seems to be a promising technique for dosimetric measurements on CT scanners when no table translation is possible.
Thirdly this project was used for a clinical comparison between the conventional pencil ionization chamber and the CTDP. The CTDP was used for measurements both during helical scanning and during axial scanning with the Mover. The pencil ionization chamber was used during axial scanning. Measuring free in air did not show the correspondence one could wish for. Quite possibly the plastic tube to give support for the CTDP was a contributing factor. When measuring in the conventional CTDI phantoms the results showed a good correspondence.
Fourthly this project evaluated how size-specific dose estimates could be used from CTDI_{vol} to more accurately know what the exposure will be for patients of different sizes. Using these size-specific dose estimates from AAPM 204 seems to be a promising way for the doctors and radiographers to more accurately know the exposure for any patient. Especially in that regard that CTDI_{vol} tends to be underestimated for small children.

Acknowledgement

Thanks to my supervisors:

- Hans Bjerke for his expertise in dosimetry, calibration procedures and having interesting ideas.
- Hilde Olerud for her expertise in CT dosimetry, positive spirit, hospitality and for being the founder of this project.
- Anne Thilander Klang for sharing her clinical expertise and both very deep and broad knowledge.

- Also many thanks to RTI Electronics AB and Lars Herrnsdorf for their support.
- Lastly, many thanks to Erlend Andersen at Sørlandet Hospital in Kristiansand for sharing a CT to this project.

References

[1] Computed Tomography — An Increasing Source of Radiation Exposure
David J. Brenner, Eric J. Hall
New England Journal of Medicine 2007; 357:2277-2284 (2007-11-29)

[2] Radiologiske undersøkelser i Norge per 2008 Trender i undersøkelsesfrekvens og stråledoser til befolkningen
Almén A, Friberg EG, Widmark A, Olerud HM
StrålevernRapport (2010-12)
(www.nrpa.no/ Publikasjoner/StrålevernRapport)

[3] Medical Electrical Equipment – Part 2-44: Particular requirements for basic safety and essential performance of X-ray equipment for computed tomography
IEC 60601-2-44 Edition 3.0 (2009-02)

[4] IAEA Technical Reports Series No. 457
Dosimetry in Diagnostic Radiology: An International Code of Practice
International Atomic Energy Agency, Vienna (2007)

[5] Computed Tomography Dose Assessment - A Practical Approach
Leitz W, Axelsson B, Szendrö G
Radiation Protection Dosimetry, Vol. 57, Nos 1-4, pp. 377-380 (1995)
Nuclear Technology Publishing

[6] Size-Specific Dose Estimates (SSDE) in Pediatric and Adult Body CT Examinations
Report of AAPM task group 204 (2011)

[7] The trouble with CTDI100
Boone JM
Med. Phys. 34, 1364-1372 (2007)

[8] Comprehensive Methodology for the Evaluation of Radiation Dose in X-ray Computed Tomography
A New Measurement Paradigm Based on a Unified Theory for Axial, Helical, Fan-Beam, and Cone-Beam Scanning With or Without Longitudinal Translation of the Patient Table
Report of AAPM task group 111: The future of CT Dosimetry (2010)

[9] A new look at CT dose measurement: Beyond CTDI
Dixon RL
Med. Phys. 30 (6), (June 2003)

[10] Medical diagnostic X-ray equipment – Radiation conditions for use in the determination of characteristics
IEC 61267 Second Edition (2005-11)

[11] Evaluation of measurement data-
-Guide to the Expression of Uncertainty in Measurement
JCGM 100:2008

[12] Manual for the CT Dose Profiler by RTI Electronics Inc.
CT Dose Profiler User's Manual - English - Version 5.1A. (september 2012)

[13] Review of Methods to Control Patient Doses and Image Qualty in Various CT Techniques.
Lars Herrnsdorf
Proceedings of the International Conference "Medical Physics 2012" 8 - 10 November 2012, Kaunas, Lithuania

[14] Discovery^{TM} CT750 HD
Technical Reference Manual, English
5432432-1EN, Revision: 1 (2012)

[15] Evaluation of two thin CT dose profile detectors and a new way to perform QA in a CTDI head phantom
Cederquist Björn
Master Degree Thesis, University of Gothenburg, (2008)

[16] X-ray mass attenuation coefficients in PMMA
http://physics.nist.gov/PhysRefData/XrayMassCoef/ComTab/pmma.html

Appendix A

The uncertainties associated with the calibration procedure was evaluated according to, 'Guide to the Expression of Uncertainty in Measurement' (GUM), [11]. It was evaluated in three steps. Firstly, factors influencing due to radiation field, set-up and calibration. Secondly, factors influencing the use of the reference chamber. Thirdly, factors influencing the use of the detector for calibration.
Some uncertainties are known, so called Type A uncertainties according to GUM. Some uncertainties can not exactly be known and a scientific judgement needs to be made, this is called Type B uncertainties according to GUM. Often Type B uncertainties are estimated to have a uniform distribution of uncertainty, often called a rectangular distribution. Also a triangular distribution of uncertainty can be assumed.

All uncertainties associated with the calibration procedure was calculated according to the following equation:

$$\mathrm{U} = \mathrm{K} \cdot \sqrt{\sum^{i} {u_i}^2} \tag{18}$$

where the square root of the quadratic sum for all influencing factors u_i was multiplied with a coverage factor (also called K-factor in GUM [11]). The K-factor in this project was, K=2, which results in a confidence interval of approximately 95%.

In the following page, it can be seen how the uncertainties associated with the calibration of the CTDP was evaluated. In several cases a scientific judgement was made for Type B uncertainties. A rectangular or a triangular distribution was assumed. Denoted (R) or (T) in the following page. (N) is the denotation for a normal distribution.

X-ray Kerma Length Product (KLP) **Uncertaintybudget Doslab NRPA**

Utarbeidet av	Rev. Nr./Dato	Dokument nr.
Hans Bjerke	2013-05-18	V-3-09-02

	Source of uncertainty	Quantity X_i	Estimate x_i	Deviation u_c	rel. st. uncert. $u(x_i)$	Prob. dist.	Sens. Coeff. c_i	$u(x_i)$ %
1	**Factors due to radiation field, set-up and calibration:**							
1,1	X-ray output stability	k_{stab}	1	0,0015	0,0015	N	1	0,15
1,2	Differences in energy spectra of radiation beams	k_{spec}	1	0,0009	0,0005	R	1	0,05
1,3	Field inhomogeneity	k_{inhom}	1	0,0000	0,0000	N	1	0,00
1,4	Uncertainty of the calibration coefficient reported by PSDL	N_{KL}	26,13	0,2221	0,0085	N	1	0,85
1,5	Constancy of the calibration coefficient		26	0,0700	0,0027	N	1	0,27
	Quadratic sum							0,82
	Combined uncertainty						$u_c(y)$ %	0,91
2	**Factors influencing use of the reference standard:**							
2,1	Current	**I [A]**	6,66E-11	---	3,02E-04	N	1	0,03
2,2	Leakage	**I [A]**	6,66E-11	7,18E-16	1,08E-05	N	1	0,00
2,3	Recombination	k_s	1	0,0035	0,0020	R	1	0,20
2,4	Polarity effect	k_{pol}	1	0,005	0,0029	R	1	0,29
2,5	Temperature (K)	**T**	300	0,1000	0,0002	R	1	0,02
2,6	Pressure (kPa)	**p**	101,3	0,0100	0,0001	R	1	0,01
2,7	Humidity	k_h	1	0,001	0,0006	R	1	0,06
2,8	Chamber orientation		1	---	0,0012	R	1	0,12
2,9	Reproduction of source to chamber distance	**d [cm]**	100	0,2	0,0008	T	1	0,08
2,10	Reproduction of irradiated length (5 cm).		5,1	0	0,0000	R	1	0,00
	Quadratic sum							0,15
	Combined uncertainty						$u_c(y)$ %	0,39
3	**Factors influencing use of the chamber for calibration**							
3,1	Product readout	P_k	1,19	3,52E-05	2,95E-05	N	1	0,00
3,2	Constancy of Calibration factor on two different days	N_K	1,19	0,0052942	0,0031	R	1	0,31
3,3	Leakage		0	0	0	N	0	0,00
3,4	Recombination	k_s	1	0,0035	0,0020	R	0	0,00
3,5	Polarity effect	k_{pol}	1	0,005	0,0029	R	0	0,00
3,6	Temperature (K)	**T**	300	0,1000	0,0002	R	0	0,00
3,7	Pressure (kPa)	**p**	101,3	0,0100	0,0001	R	0	0,00
3,8	Humidity	k_h	1	0,001	0,0006	R	0	0,00
3,9	Chamber orientation		---	---	0,0012	R	1	0,12
3,10	Reproduction of source to chamber distance	**d [cm]**	100	0,2	0,0008	T	1	0,08
3,11	Reproduction of irradiated length (5 cm).		5,102	0,1	0,0113	R	1	1,13
	Quadratic sum							1,40
	Combined uncertainty						$u_c(y)$ %	1,18
4	**Total uncertainty**							
	Quadratic sum							2,37
	Combined uncertainty						$u_c(y)$ %	1,54
	Expanded uncertainty (k=2)							3,08